Festschrift zum 60. Geburtstag von Helfried Mostler
Geol. Paläont. Mitt. Innsbruck, ISSN 0378–6870, Bd. 20, S. 283–311, 1995

CONTROLS ON THE DIAGENESIS OF UPPER TRIASSIC CARBONATE RAMP SEDIMENTS: STEINPLATTE, NORTHERN ALPS (AUSTRIA)

Erik Flügel & Roman Koch

With 11 figures and 4 plates

Abstract:
The Steinplatte near the Austrian-German boundary was long regarded to be a classical model for Upper Triassic reefs formed at carbonate platform margins. This model was replaced by a distally-steepened ramp model (STANTON & FLÜGEL (1989, 1995). Our paper discusses the early diagenetic criteria of the 'mound facies' of the Oberrhätkalk exposed in three sections in the western and southern cliff walls. The mound facies consists of three aggradational depositional cycles separated by regressive phases. Primary facies differences within these cycles resulted in the formation of complex hydrological systems acting as flow pathways for marine and/or meteoric or altered pore waters and producing different carbonate cement types.
The flow pathways were intensified by repeated early meteoric influx causing dissolution of mineralogically unstable bioclasts (predominantly mollusks). Increasing access of pore waters resulted in the formation of molds and vugs and recrystallization of great parts of the rocks above and below the beds which acted as pore water conduits. Marine pore waters resulted in the abundant formation of radiaxial-fibrous calcite cements whose growth was strongly substrate-controlled. Interruptions of cement growth by reddish silt and vadose silt point to subaerial exposure and karstification of adjacent platform areas.
The 'mound facies' of the Steinplatte is an example of a complex cementation pattern controlled by (1) the spatial distribution of primary facies criteria (matrix, grains, porosity types), (2) deposition on a ramp, causing variations of the hydrological systems in time, and (3) local substrate control favoring the precipitation of radiaxial-fibrous calcite cement within a marine diagenetic environment.

Zusammenfassung:
Die Steinplatte bei Waidring, nahe der österreichisch-deutschen Grenze, galt lange als klassisches Modell für obertriadische Plattformrand-Riffe. Diese Vorstellung wurde durch STANTON & FLÜGEL (1989, 1995) durch das Modell einer distal versteilten Karbonatrampe ersetzt. In der vorliegenden Arbeit werden die frühdiagenetischen Merkmale der in drei Profilen der Steinplatte-West- und Südwand untersuchten „Mound Fazies" des Oberrhätkalkes diskutiert. Die Mound Fazies besteht aus drei aggradierenden Ablagerunszyklen, die durch regressive Ereignisse beeinflußt werden. Primäre Faziesunterschiede innerhalb dieser Zyklen waren für die Entstehung komplexer hydrologischer Systeme verantwortlich, durch welche die Möglichkeiten und die Intensität des Zutritts von marinen und/oder meteorischen sowie in ihrem Chemismus veränderten Porenwässern gesteuert wurden.
Wiederholter Zutritt von Süßwasser führte zur Lösung mineralogisch instabiler Bioklasten (überwiegend Mollusken), die in „Shell Beds" angehäuft sind. Derart kam es zur Bildung von Lösungsporen und zur Rekristallisation der Schichten im Liegenden und Hangenden der den Porenwasserfluß ermöglichenden Schichten. Wiederholte Wechsel zu marinen Porenwässern führten zur Bildung von radiaxial-fibrösen Kalzitzementen, deren Entstehung in hohem Maß substratgesteuert erscheint. Unterbrechungen der marinen Zementbildung durch Auftauchen und Verkarstung benachbarter Plattformareale werden durch Einschaltungen von vadosen Kristallsilten und Hämatitsäumen angezeigt.
Die Mound Fazies der Steinplatte stellt ein ausgezeichnetes Beispiel für die Enstehung eines komplexen Zementationsmusters im Bereich eines Hanges dar. Lösung und Zementation wurden durch die räumliche Verteilung der Primärfazies (Matrix, Komponenten, Porentypen), durch eine in Aggradationszyklen ablaufende Sedimentation am Hang einer Rampe, durch die dadurch bedingten und in der Zeit wechselnden hydrologischen Systeme sowie durch die Substratabhängigkeit der im Oberrhätkalk quantitativ dominierenden radiaxial-fibrösen Zemente gesteuert.

1. Introduction

The Steinplatte, near Waidring in Northern Tyrol (fig. 1), was long considered to be a classical model for Upper Triassic reefs formed at carbonate platform margins (OHLEN, 1959; ZANKL, 1971; LOBITZER, 1980; PILLER, 1981). This model was replaced by STANTON & FLÜGEL (1989, 1995), who favored a ramp model. They explained the Steinplatte as an accretionary, distally steepened ramp developing from a homoclinal ramp and composed predominantly of carbonate bioclastic sands with patchy coral and '-calcisponge' buildups.

This paper describes and discusses the diagenetic criteria of the 'mound facies' of the Oberrhätkalk exposed in three sections in the western and southern cliff walls (figs. 2, 3). The sections C, B and A document significant lateral and vertical changes in the composition of the sediment along a basinward steepened slope dipping 20°–30° W (fig. 3). Marker beds (e.g. the 'White Bed', several 'shell beds', marly intercalations as well as the relative amount of matrix, grains and grain types) allow depositional units

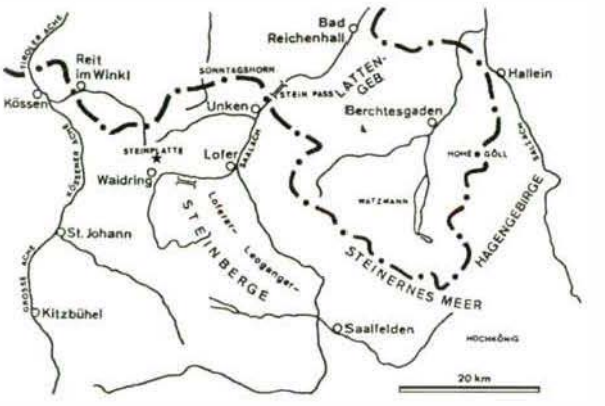

Fig. 1: Location of the Steinplatte near the Austrian/German boundary. The Steinplatte lies approximately 70 km SE München and 30 km SW Salzburg.

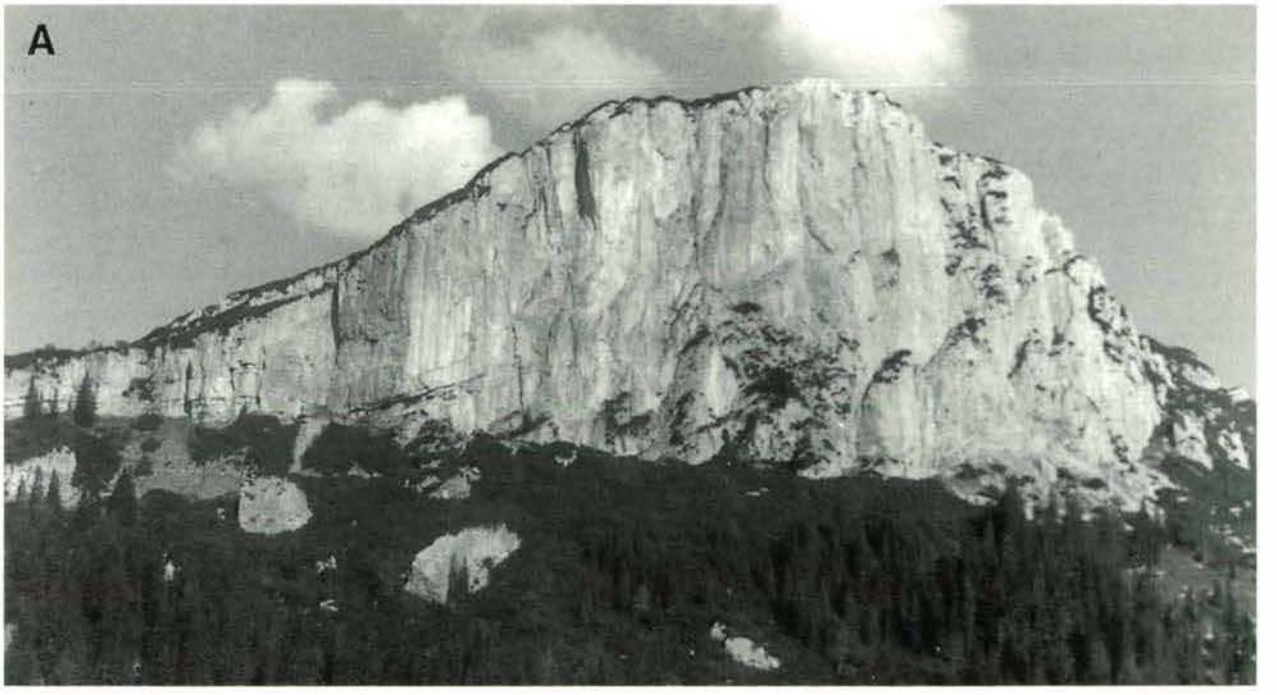

Fig. 2: Study area. **A** Western cliff wall of the Steinplatte. The photograph, taken from the Grünwaldkopf, exhibits the bedded and massive Kössen beds grading laterally and vertically into the limestone of the Steinplatte ('Oberrhätkalk'). Distinct downslope bedding is visible in the transitional area between Oberrhätkalk and flat lying Kössen beds. The cliff comprises the 'mound facies' (about 150 m) which is overlain by the onlapping beds of the thin 'capping facies' on the flank of the Steinplatte (visible at the top left). The capping facies includes the 'coral gardens' on the northern slope of the Steinplatte and the eastern slope of the Plattenkogel. **B** Sketch showing the location of the sections studied A (route 5), B (route 12) and C (route 21). The 'White Bed' dipping about 20° west is dotted. Modified from STANTON & FLÜGEL (1989).

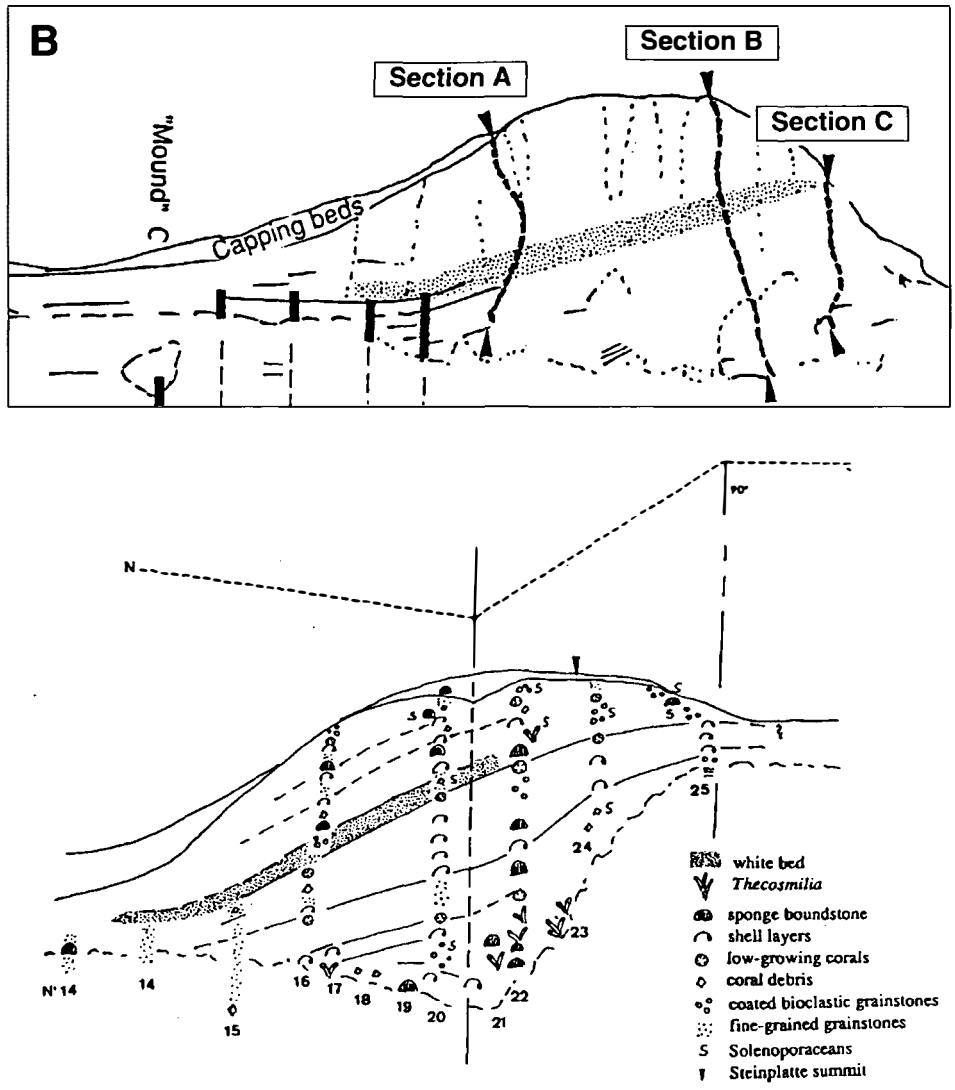

Fig. 3: Distribution of facies criteria within the mound facies. Numbers refer to sampling localities. Lateral and vertical distances are not to scale. The carbonate ramp (right) becomes distally steepened in the vicinity of section D (locality 24) and changes into a distinct slope marked by shell bed III and the 'White Bed'. Note the changes in the thickness of shell bed III (shell symbol; about 25 m in the Wieslochsteig section (locality 25), 8 m in section D, 26 m in section B and 5 m in section A). Boundstones are more common in section C and in the beds overlying the 'White Bed'. Modified from STANTON & FLÜGEL (1989).

to be correlated (fig. 4) reflecting changes in sea-level and in early diagenetic patterns (figs. 9–11).

The mound facies is predominantly composed of fine- and medium-grained bioclastic and lithoclastic carbonate sands, shell coquinas and some thin, small-scaled autochthonous boundstone structures. Boundstones with sponges, corals and solenoporacean algae are mainly restricted to section C. The sections B and A exhibit wacke-, pack- and grainstones varying in composition, frequency of grains and matrix content over the ramp towards the basin (see STANTON & FLÜGEL, 1989). Marine cements as well as meteoric diagenetic features can be recognized in all the sections, providing an insight into the relationships between cementation and

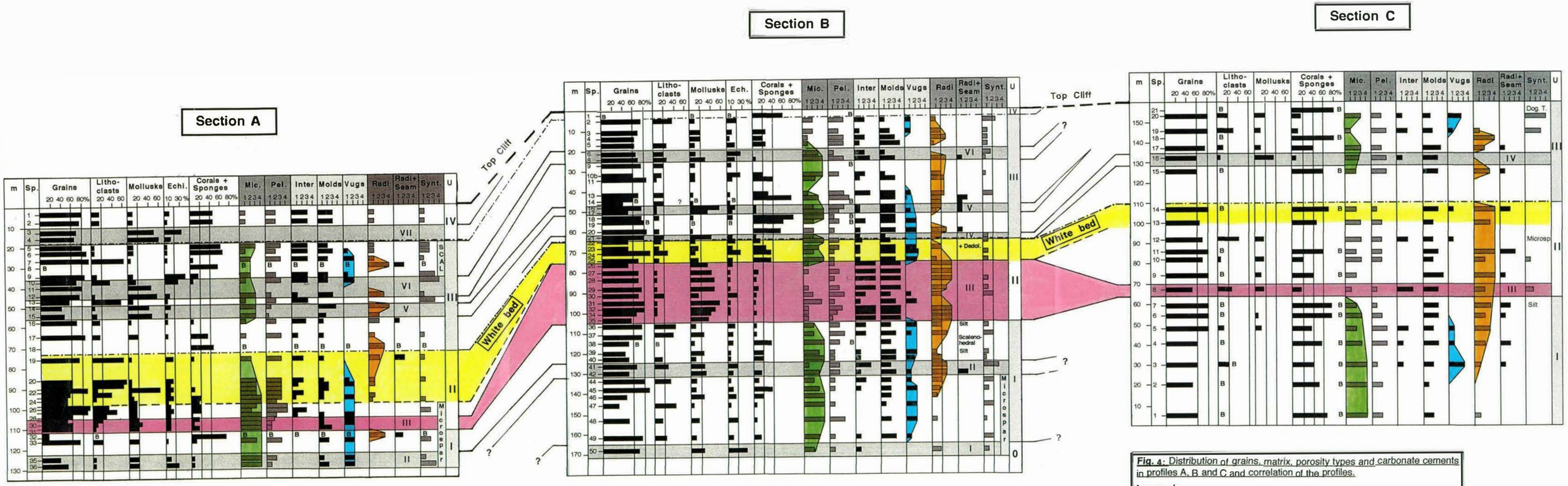

Fig. 4: Distribution of grains, matrix, porosity types and carbonate cements in profiles A, B and C and correlation of the profiles.

Legend:

Sp.	- Sample
Mic.	- Micritic matrix
Pel.	- Peloidal matrix
Inter	- Interparticle porosity
Radi	- Radiaxial-fibrous cements
+Seam	- RFC separated by reddish-dusty layers
Synt.	- Syntaxial overgrowth
Microsp.	- Microsparitic matrix (recrystallized)
Scal.	- Scalenohedral calcites
U	- Unit

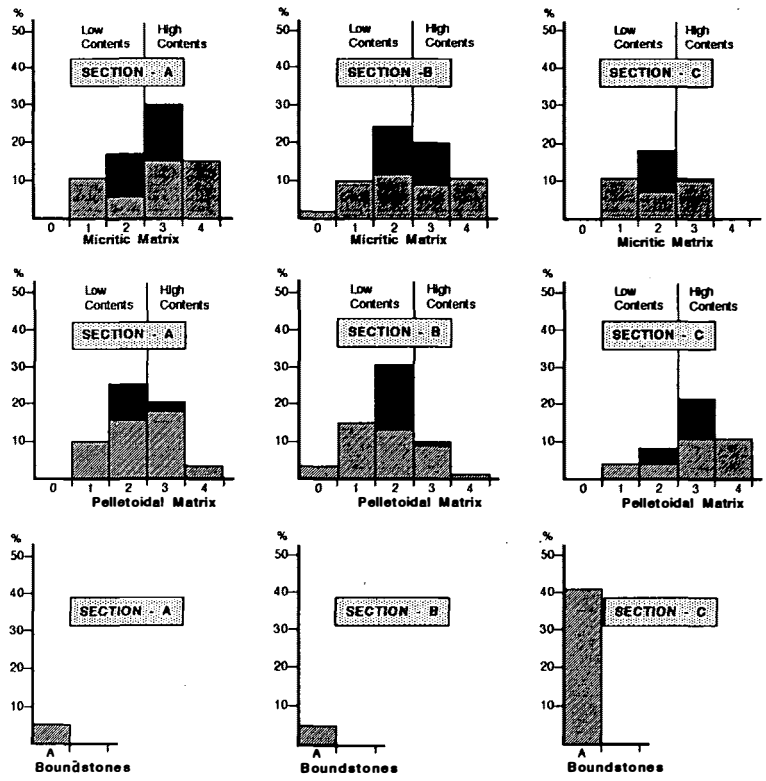

Fig. 5: Frequency of micrite matrix, peloidal matrix and boundstones in the sections A, B and C. The numbers indicate estimated frequencies: 0 = absent, 1 = rare, < 5%, 2 = common, 5-10%, 3 = abundant, 10-20%, 4 = very abundant, > 20%. The histograms are summarized as black bars; 'low' and 'high' contents correspond to rough estimations.

present in section A whereas section B exhibits low amounts. Peloids in section C seem to be related to organic activity, the peloids of section A may correspond to small micritic intraclasts.

The differentiation of the mound facies into depositional units facilitates the recognition of diagenetic patterns and their controls by sea-level fluctuations (fig. 4).

The lowermost **unit-0** is of minor importance for our study. It occurs only in section B and is represented by shell bed I (sample B 50). About 70% of the grains are mollusk and echinoderm debris.

The overlying **unit-I** can be recognized in all the sections (section C: samples 1–7; section B: samples 49–36; section A: samples 36–32). It comprises the interval between shell bed I and the base of shell bed III, including shell bed II.

In all three sections unit-I is characterized by a very high amount of micrite matrix (figs. 4 and 6). Grain frequency decreases slightly from east to west (fig. 6). Most grains in section C are angular coral fragments. About 60% of the samples of section B and more than 75% of the samples from section A exhibit grain frequencies of less than 60% of the rock volume, indicating a mixture of autochthonous sediment production and downslope sediment input. Differences in the frequency of peloidal matrix (common in section A, less common in section B) may be explained by a different origin of the peloids as mentioned above. Mollusk grains are rare in section C and more frequent in section B, together with echinoderm fragments. Corals are rare within the slope sediments except for one bed underlying shell bed III (section B: sample 38; section A: sample 32).

the composition of the depositional units, matrix content and grain types controlling the cement stratigraphy.

2. Material and methods

The study is based on 107 thin sections from three profiles (A: 36 samples, B: 50 samples, C: 21 samples) covering a thickness of about 150 meters (fig. 3). The thin sections were studied with regard to rock bulk composition, porosity types and cement types. Because the available grain bulk data (STANTON & FLÜGEL, 1989) proved to be insufficient for evaluating the controls of sediment composition on cementation, rock bulk compositional data were estimated. This includes the number of grains, the amount of matrix, and the frequency of lithoclasts (predominantly reworked micrite), mollusks (predominantly pelecypods), echinoderms as well as 'potential reefbuilding organisms' (corals and sponges; see figs. 3 and 4).

The amount of matrix, pores (minus-cement porosity) and cement types was estimated semiquantitatively (see fig. 4).The scale used is: 0 = absent, 1 = rare, < 5%, 2 = common, 5–10%, 3 = abundant, 10–20%, 4 = very abundant, > 20%. Percentages correspond roughly to rock bulk composition. Two matrix types were distinguished (micrite matrix and peloidal matrix) because they reflect differences in permeability. Pores are differentiated into primary interparticle pores, molds and vugs. Estimating the matrix content, boundstones were not taken into consideration separately.

The prevailing cements occurring in the carbonate sands correspond to radiaxial-fibrous, syntaxial and granular types. Radiaxial-fibrous cements can be subdivided into those consisting of only one generation of cement crystals and those consisting of several generations. Granular cements were not studied in detail because the current paper focuses on microscopic analysis and does not include the stable isotope and cathodoluminescence data necessary for explaining these cement types.

All data are summarized in fig. 4 which shows the correlation chart of the three sections. The distribution of grains, peloidal matrix and micrite matrix of the depositional units of the Steinplatte 'mound facies' is shown separately in figs. 5–8. The most important cement types forming the basis for our interpretations are documented in plates 1– 4.

3. Correlation and subdivision of the Steinplatte ramp sediments

A correlation of the cliff wall sections A, B and C, based on textural and diagenetic criteria (fig. 4), supports the depositional model developed by STANTON & FLÜGEL (1989, 1995). The overall sedimentation pattern corresponds to that of a laterally prograding, distally steepened carbonate ramp exhibiting *five depositional units*. These units are characterized by different amounts of grains and matrix:

The number of grains decreases from east to west (fig. 4), showing characteristic lateral patterns within units-I, -II and -III, which are also reflected by the amount of micrite matrix (fig. 5). Low grain contents coincides with high matrix content and vice versa. The overall trend is characterized by an increase in the amount of micrite matrix from east to west (fig. 5). Low amounts of micrite (grades 1 and 2) and some moderate amounts (grade 3) occur in section C. Micrite content increases in section B, exhibiting the highest grades (3 and 4) in the basinward section A. Peloidal micrite matrix is most common in section C and co-occurs with boundstones. High amounts of peloidal micrite are also

Fig. 4: Distribution of grains, matrix, porosity types and carbonate cements in the sections A, B and C and correlation of the sections.

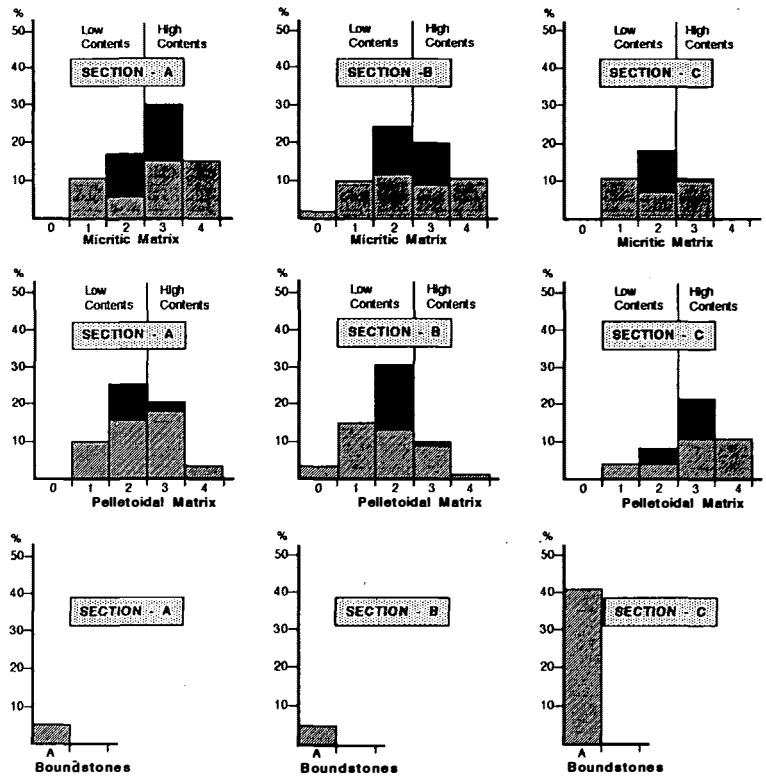

Fig. 5: Frequency of micrite matrix, peloidal matrix and boundstones in the sections A, B and C. The numbers indicate estimated frequencies: 0 = absent, 1 = rare, < 5%, 2 = common, 5-10%, 3 = abundant, 10-20%, 4 = very abundant, > 20%. The histograms are summarized as black bars; 'low' and 'high' contents correspond to rough estimations.

present in section A whereas section B exhibits low amounts. Peloids in section C seem to be related to organic activity, the peloids of section A may correspond to small micritic intraclasts.

The differentiation of the mound facies into depositional units facilitates the recognition of diagenetic patterns and their controls by sea-level fluctuations (fig. 4).

The lowermost **unit-0** is of minor importance for our study. It occurs only in section B and is represented by shell bed I (sample B 50). About 70% of the grains are mollusk and echinoderm debris.

The overlying **unit-I** can be recognized in all the sections (section C: samples 1–7; section B: samples 49–36; section A: samples 36–32). It comprises the interval between shell bed I and the base of shell bed III, including shell bed II.

In all three sections unit-I is characterized by a very high amount of micrite matrix (figs. 4 and 6). Grain frequency decreases slightly from east to west (fig. 6). Most grains in section C are angular coral fragments. About 60% of the samples of section B and more than 75% of the samples from section A exhibit grain frequencies of less than 60% of the rock volume, indicating a mixture of autochthonous sediment production and downslope sediment input. Differences in the frequency of peloidal matrix (common in section A, less common in section B) may be explained by a different origin of the peloids as mentioned above. Mollusk grains are rare in section C and more frequent in section B, together with echinoderm fragments. Corals are rare within the slope sediments except for one bed underlying shell bed III (section B: sample 38; section A: sample 32).

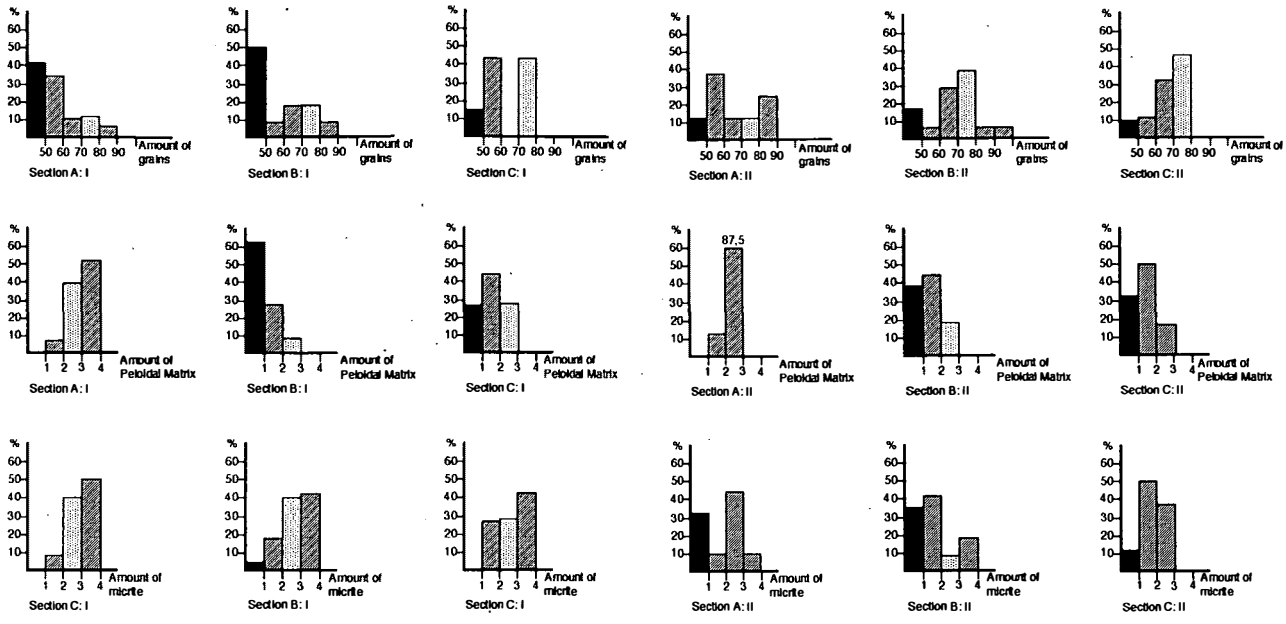

Fig. 6: Frequency of grains and matrix types within rock unit-I in sections A, B and C. For legend see Fig. 5.

Fig. 7: Frequency of grains and matrix types within rock unit-II in sections A, B and C. For legend see Fig. 5.

Unit-II contains the most conspicuous coquina (shell bed III) and the 'White Bed', and is overlain by shell bed IV belonging to unit-III. Shell bed III and the 'White Bed' occur in all three sections but because the overlying shell bed IV is missing (or was not sampled) in section A, the boundary between unit-II and unit-III may be fixed at the base of shell-bed V, at the same position as in section B, or slightly deeper below a boundstone (section A).

In contrast to unit-I, unit -II is characterized by very low amounts of micrite matrix (especially in section B), the highest numbers of grains, highest numbers of mollusk shells and echinoderm fragments (figs. 4 and 7) as well as by large amounts of radiaxial-fibrous cements (fig. 4). Bioclastic grains are predominantly mollusks within shell bed III and echinoderm and coral debris in the 'White Bed'. The bulk of the 'White Bed' is characterized by bioclastic/lithoclastic pack- and grainstones which differ significantly in the small grain size from other parts of the mound facies. Lateral changes within unit-II (fig. 7) concern the amount of micrite matrix (slightly increasing from east to west), the frequency of peloidal matrix (moderate in section C, higher in sections B and A), the number of grains (slightly decreasing towards the basin) and the proportion of grains within the 'White Bed'. These lateral changes within unit-II do not affect overall grain frequency and interparticle porosity, which are very high in all the sections.

Unit-III comprises the interval between shell bed V and the base of shell bed VII (exposed only in section A). It includes the shell beds V and VI as well as the intercalated sediments. The unit is characterized by larger amounts of micrite matrix, varying slightly vertically (high in the lower and upper part, low in the central part of the sections) but remaining rather constant laterally (fig. 8). The central part is characterized by larger amounts of echinoderms (section A) and corals and sponges (sections B and C). Mollusk shell debris is predominantly restricted to the shell beds, coral debris to the intercalated sediments. The bulk frequency of grains and of peloidal matrix decreases slightly basinwards.

The uppermost **unit-IV** is present only in the sections A and B and includes shell bed VII of

section A. Micrite matrix is low in both sections, peloidal matrix decreases slightly from east to west.

4. Depositional model: Aggradational cycles controlled by sea-level fluctuations

4.1 Shell beds

Shell beds I to VII, used as marker horizons, are characterized by large amounts of pelecypod and brachiopod shells, and sometimes frequent echinoderm fragments. Other bioclasts are rare. Shell beds occur both in units rich in micrite (units-I and -III) and in units poor in micrite (units-II and -IV). The shell beds (except for shell bed I, IV and VII) can be followed downslope to the basin.

Shell bed III of the lower part of unit-II is of special interest because it indicates a distinct change in the depositional pattern by having formed a depositional relief and acted as a diagenetic pathway.

This shell bed is characterized by

a) Wide lateral extension: The shell accumulation can be followed for more than two kilometers from the Kössen beds in the west to the area east of the Wieslochsteig.
b) Differences in the setting: Shell bed III developed on the slope (sections A and B) as well as on the shallow outer ramp (section D east of section C (fig. 2) and the Wieslochsteig section, about 1 km east of section C; see STANTON & FLÜGEL, 1989).
c) Marked differences in thickness: About 5 m in the downslope section A, about 26 m in slope section B, about 8 m in the outer ramp section D (transect section), and about 25 m in the outer ramp section at the Wieslochsteig.
d) Differences in the facies of the underlying and overlying beds in the western and eastern Steinplatte area: Underlying beds are boundstones; overlying beds correspond to the fine-grained sediments of the 'White Bed' in sections A and B. In section D and the Wieslochsteig underlying beds are biointraclastic echinoderm pack- and floatstones as well as grainstones and overlying sediments are bioclastic coated grainstones and wackestones.
e) Differences in sediment composition: Shell bed III corresponds to a bioclastic micritic sediment (predominantly shell/echinoderm floatstones and packstones) in sections A, D and in Wieslochsteig whereas in section B the shell bed is characterized by coarse-grained shell rudstones.

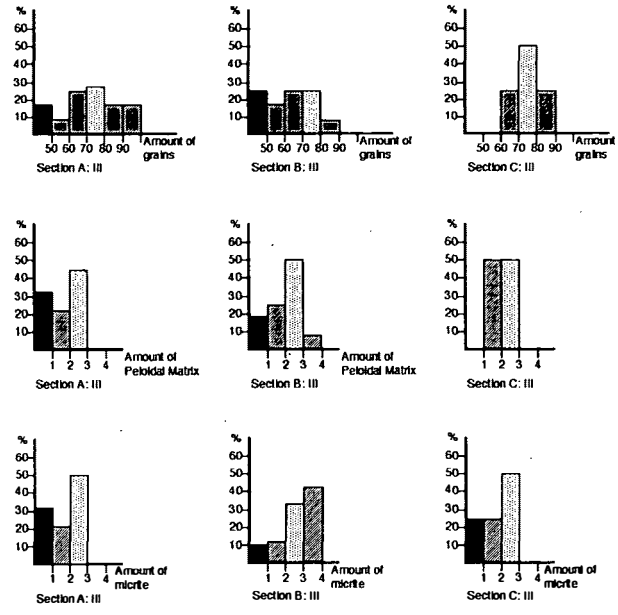

Fig. 8: Frequency of grains and matrix types within rock unit-III in sections A, B and C. For legend see Fig. 5.

Shell bed III is a good example of a *'fossil concentration'*. The term was coined for a 'relatively dense accumulation of biological hardparts, irrespective of taxonomic composition, state of preservation, or degree of post-mortem modification' (KIDWELL et al., 1986). Following the conceptual framework developed for the analysis and classification of these skeletal concentrations, shell bed III corresponds to 'mixed biogenic/sedimentological concentration'. Biogenic and sedimentologic contributions in the formation of the shell bed were different at the

various sites as shown by a comparison of the taxonomic composition, biofabric, geometry and internal structure of shell bed III:

1) Taxonomic composition: The concentrations are polytypic at all sites. They consist of several types of skeletons. This includes the groups taking part in the formation of the shell bed (pelecypods, echinoderms, brachiopods, gastropods) as well as the differences on the generic level within the pelecypods.
2) Biofabric: The three-dimensional arrangement of the skeletal elements is different at different sites. Shells are predominantly matrix-supported in sections A and D and the Wieslochsteig in contrast to the thick shell bed of section B, which is characterized by bioclast-support. Sorting is poor at all sites but significantly poorer in sections B and D and the Wieslochsteig section. Samples from these sections exhibit oblique and perpendicular orientations of shells in cross sections. Packing varies at different sites, it is low in samples from section A but high in samples from sections B and D.
3) Geometry: Shell bed III exhibits a wedge-shaped geometry on the slope (sections A and B). On the ramp, however (section D and the Wieslochsteig), the shell bed corresponds to a 'bed' (in the terminology of KIDWELL et al., 1986) exhibiting considerable variations in thickness (5 to about 25 m) over a lateral distance of about 500 meters.
4) Internal structure: Shell bed III corresponds to 'simple concentrations' defined by an internally homogenous composition. This is especially evident within the thick concentrations in section B and the Wieslochsteig. Vertical or lateral internal variations pointing to the existence of shelly turbidites or offshore tempestites (AIGNER, 1982, 1986) are absent.

Using the ternary diagram proposed by KIDWELL et al. (1986) to describe the concentrating processes of fossil accumulations, the shell bed of section A falls into field 4, section B and section D into field 2, and the shell bed of the Wieslochsteig section into fields 4 and 1. Field 1 characterizes autochthonous and parautochthonous biogenic concentrations (indicated in the lower part of the Wieslochsteig shell bed by abundant pelecypods preserved in living position). Field 2 describes concentrations predominantly caused by hydraulic effects and/or variations in the sedimentation. Field 4 characterizes concentrations formed by an interplay of sedimentologic and biogenic processes.

Along an onshore-offshore transect sedimentological concentrations should decrease in abundance towards the basin, because of diminishing water energy at the sea floor, assuming constant sediment accumulation rates across the transect. Sedimentological shell concentrations may be typical in various environments (including beach, tidal flat, lagoon, shoals and inner shelf settings). In the model developed by KIDWELL et al. (1986), the Wieslochsteig section shell bed would correspond to a 'lagoonal' position, the section D to shoals and sections B and A to inner shelf positions below fair weather waves but above the storm wave base. Parautochthonous shell associations occur only in the Wieslochsteig section.

Unfortunately, the taxonomic composition of shell bed III and other shell beds is not well known (HAHN, 1910: VORTISCH, 1926; PILLER, 1981). However, by attributing the recorded pelecypod genera to the ecological groups distinguished by KAUFFMAN (1969), the primary habitats of the bivalves can be inferred. Most of the recorded pelecypod genera are members of epifaunal hard bottom communities and include byssate free-swinging bivalves (*Oxytoma, Pteria, Rhaetavicula*), byssate fissure- and cavity dwellers (*Lima*) as well as cemented epifaunal bivalves (oysters, *Plicatula, Atreta*). Most of these genera prefer firm or hard substrates and were suspension feeders living in shallow high-energy environments. Members of soft bottom communities are represented by *Modiolus, Gervilleia* and *Hoernesia*.

Many of these genera also occur in the bivalve biofacies types of the Kössen Beds of the Steinplatte area (GOLEBIOWSKI, 1991). Here the

coquina beds of the lower part of the Hochalm Member, corresponding to proximal tempestites of a shallow carbonate ramp, are concentrated at the base of transgressive cycles. A similar situation may be assumed for some of the shell beds within the mound facies of the Steinplatte (e.g. shell bed III and shell bed VII).

Any explanation of Shell Bed III must take into account the following points:

1) The primary habitats of the pelecypods were shallow, high-energy environments providing firm and hard bottom substrates.
2) All the sites of shell bed III except the Wieslochsteig area exhibit allochthonous fossil concentrations.
3) These concentrations were caused by hydraulic effects acting on the slope as well as on the shallow outer ramp.
4) Thickness variations of the shell bed are similar on the slope and on the ramp.
5) The allochthonous shell material was deposited in low energy environments at the slope as well as on the ramp.
6) Section B (shell rudstone) is a remarkable exception which may indicate by-passing of mud or the existence of local high-energy conditions caused by currents.

KIDWELL & AIGNER (1985) recognized three pathways in the formation of complex shell accumulations: (1) Continuous accumulation of shells because sedimentation fails to keep up with hardpart accumulation. This may result from a) a negligible sediment supply or bypassing of sediment, b) high biological production, or c) an abundant supply of allochthonous hardparts from outside. (2) No or low background sedimentation relative to hardpart accumulation, interrupted by rapid deposition of muddy sediment. This allows a colonization by burrowing infauna which contributes to the formation of firm substrates for further shells. (3) Episodes of erosional reworking of soft-bottom colonizers into shell gravel lags, providing opportunities for colonization by epifaunal taxa.

The dominance of epifaunal pelecypods argues against pathway 3 and possibly also pathway 2. Continuous accumulation of shells caused by high biological production and low sedimentation is a reliable explanation for the Wieslochsteig shell bed where ecologically different epifaunal bivalves may have accumulated due to low sedimentation rates and small-scale in situ reworking (cf. FÜRSICH, 1978). The allochthonous shell bed of section B, however, could correspond to accumulations of shell gravels near the toe-of-the-slope. Here, bottom currents can concentrate allochthonous material derived from the upper part of the slope.

The formation of shell bed III was probably a regional event: The shell bed III was formed at different water depths and at different energy levels. It overlies coated grainstones (Wieslochsteig and section B) as well as wackestones, packstones and boundstones (section D and A) pointing to a widespread and rapid change in depositional conditions at the base of the shell bed. This change is also evident in other outcrops of the 'Oberrhätriffkalk', especially in the Rötelwand (SIEBER, 1937; SCHÄFER, 1979): Here, micritic carbonates with pelecypod beds and small coral patches provide the base for pelecypod coquinas, forming a shell bed up to 30 meters in thickness. This parautochthonous shell bed is overlain by different facies types; the fine-grained 'detritus mud facies' at the leeward flank of the Rötelwand structure is lithologically similar to the 'White Bed' of the Steinplatte.

4.2 Aggradational cycles

The depositional pattern on the slope of the Steinplatte and at the margin of the ramp is characterized by at least three 'aggradational cycles' which started after deposition of unit-0 with the **first cycle** comprising unit-I and unit-II. Lateral aggradation is indicated by the varying thicknesses of shell bed II and shell bed III as well as

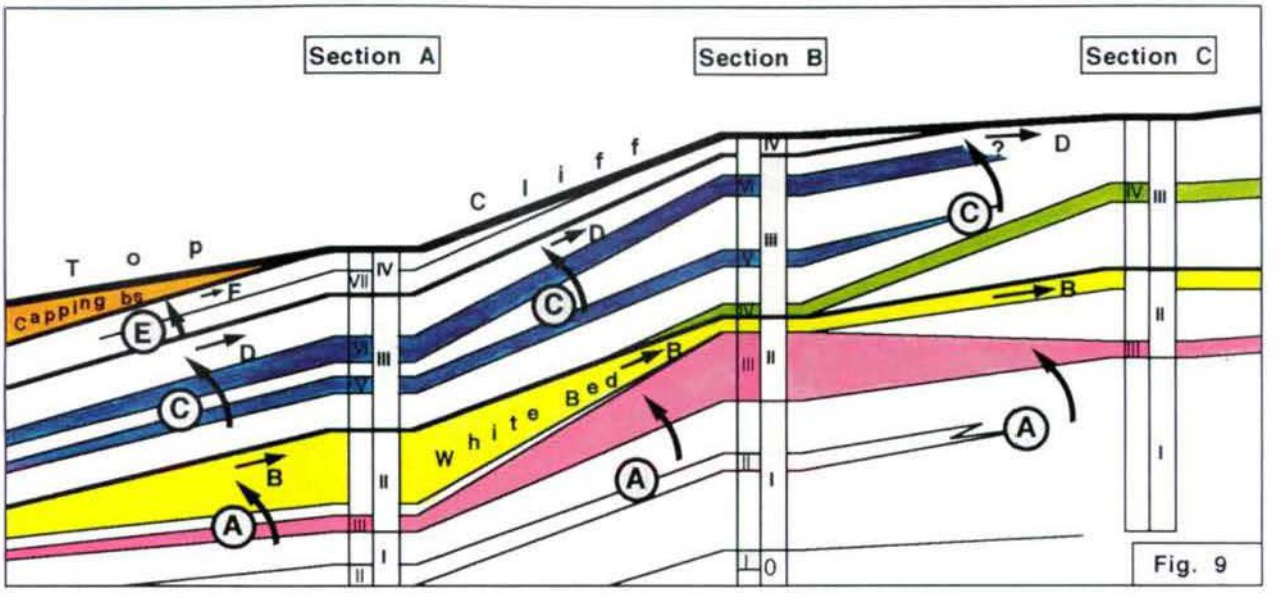

Fig. 9: Sketch of the depositional units and aggradational cycles of the distally steepened part of the carbonate ramp (mound facies). Letters refer to depositional cycles and regression events. Roman numbers (0, I, II, III, IV) within the columns to depositional units and Roman numbers at the left of the columns (I to VII) to shell beds. After the first cycle (A) a marked regression (B) took place. The second cycle (C) is characterized by shell bed III and the 'White Bed', corresponding to transgressive phases. (D) marks a regressive event. The third cycle (E) characterized by increasing shallowing of the depositional area is also terminated by a regression event (F). The decrease in the thickness of the cycles indicates decreasing aggradational deposition within a predominantly regressive megacycle characterizing the total of mound facies and capping facies.

of the 'White Bed'. The 'White Bed' was deposited within a relief of shell bed III (fig. 9). Shell bed II seems to pinch out against the more autochthonous sediments of the section C.

The boundary between shell bed III and the 'White Bed' marks the beginning of a transgressive phase. The top of the 'White Bed' may correspond to a regressive phase, characterized by low depositional rates (as indicated by hematite dust on fibrous cement calcites). The depositional gap becomes more evident from the absence of sediments: The interval between the 'White Bed' and shell bed IV of section C is only slightly developed in section B and is absent in section A.

The **second cycle** corresponds to unit-III, and ranges from shell bed IV or from the top of the 'White Bed' to the base of shell bed VII. In section B the cycle comprises the shell beds V and VI and may even extend up to a few meters above shell bed VI. In section C the second cycle is represented by the uppermost sediments of the section.

The depositional pattern of the second cycle is characterized by a low-relief sedimentation on a ramp without significant differences in thickness. The thickness is smaller than that of the first cycle. The upper boundary, marked by hematite dust on cement crystals, corresponds to a regression maximum.

The **third cycle** can be recognized only in sections A and B. It is characterized by shallowing-upward sequences consisting of grain-rich sediments. Corals and coral patches are more common as compared to the first and second cycles. The sediments of this cycle are disconformably overlain by the coral-rich sediments of the 'capping facies', exhibiting distinct indications of regressive phases (cf. STANTON & FLÜGEL, 1989).

5. Distribution of pore types within the depositional units

5.1 Relationships between matrix, porosity and substrate control of cementation

Precipitation of cements and dissolution of carbonate material depend on the number of ions present and on the rates at which water flows through pore spaces. Flow rates and, in turn, cementation are controlled by a) energy levels (creating 'active' or stagnant' diagenetic conditions within microenvironments, LONGMAN, 1980), b) rates of sedimentation and c) the distribution and geometry of pores.

High water agitation and low sedimentation rates will result in strong cementation (e.g., at the reef front), whereas low agitation combined with high sedimentation rates and the deposition of fine-grained sediment favors low cementation (e.g., in back-reef environments). An increase in fine-grained matrix results in decreasing flow rates; pure micrites, therefore, exhibit very low permeabilities (LIGHTY, 1985). Permeability and possible flow rates are higher in sediments with interparticle and intercrystalline pores than in sediments with moldic and intraparticle porosity. Permeability and porosity are strongly modified by pore size and the type and size ('pore throat diameter') of the interconnections between adjacent pores.

The amount of micrite and the percentage of 'minus-cement-porosity' and 'open porosity' can be used in evaluating diagenetic stages. These stages depend strongly on the primary depositional facies, i.e., the amount of mud-supported and grain-supported limestone types (DUNHAM, 1962).

Factors controlling early cementation in submarine and intertidal environments are

a) the supersaturation of sea water with respect to $CaCO_3$,
b) water temperature and salinity,
c) water energy, controlling the amount of dissolved cementing material (MARSHALL, 1983, 1986; HARRIS et al., 1985),
d) metabolic activity (photosynthesis and respiration) and disintegration of organic matter, causing both dissolution as well as precipitation of $CaCO_3$,
e) biogenic activity (boring, burrowing, biofilms) changing porosity and permeability,
f) sedimentation rates, favoring or hindering cementation,
g) permeability, and
h) the substrate of the cement crystals. Substrate control is caused by organic matter on grain surfaces influencing the nucleation and precipitation of the carbonate minerals and by the mineralogy of the host, which govern the mineralogy of the cement crystal (ALEXANDERSSON, 1972; BOROWITZKA, 1989).

Following the three-stage model developed for the precipitation of carbonate cement (BOROWITZKA, 1989) the formation of early cements (crystalline $CaCO_3$) requires a) the attainment of supersaturation in the system, followed by b) nucleation on substrates, influenced by the relative ranking of the stability of carbonate minerals. Once nucleation has taken place, c) crystal growth can occur within four stages as described by BOROWITZKA (1989), depending on the presence of sufficient Ca^{2+} ions and appropriate permeability/porosity conditions.

In the context of the Steinplatte study, differences in the oversaturation of the fluids can be estimated from the amount of carbonate cements. Controls of cementation by different substrates are indicated by the preference of specific grains, and permeability conditions can be inferred from variations in the matrix content of the sediment.

5.2 Distribution of pore types in the depositional units

The original porosity is occluded by different carbonate cements. All pore types described

below and in the plates, therefore, refer to 'minus cement porosity'. Porosity types include primary as well as secondary porosities (CHOQUETTE & PRAY, 1970). Fabric-selective porosity is much more common than non-fabric selective porosity.

The most abundant pore types in which marine cements are formed are primary interparticle pores and early diagenetic biomoldic pores, due to the dissolution of mollusk shells (fig. 4; pl. 1/4–6, pl. 2/5–6, pl. 3, pl. 4). Framework and interparticle pores as well as some shelter pores beneath shells occur in addition.

Vuggy porosity caused by the dissolution of micritic matrix and by enlargement of molds is concentrated in specific intervals of the sections. They are preferred sites for the formation of granular and syntaxial cements (pl. 1/1, 3, pl. 2/1–2, 5–6, pl. 3/3–4, pl. 4/2–3).

Specific pore types are related to specific depositional types (grainstones/packstones and wackestones) within the sections and occur in vertical order, pointing to an early diagenetic formation of porosity types and specific cements coeval with the formation of the depositional units I to IV.

6. Carbonate cements

The following description of carbonate cements, based on microscopic analysis only, is limited to the quantitatively most important types. Even though cathodoluminescence and geochemical data are not yet available, the differentiation of cement types, their comparison with similar cements described by BRICKER (1971), LONGMAN (1980), HARRIS et al. (1985), PREZBINDOWSKI (1985), RICHTER (1988) and TUCKER & WRIGHT (1990) as well as the recognition of distributional patterns allow a discussion of the major controls of the formation of the cements (primary facies, substrate for nucleation of cements and poroperm criteria of the sediment).

The main cement types of the Steinplatte ramp carbonates are (1) radiaxial-fibrous calcites (RFC), (2) syntaxial overgrowth on echinoderm fragments, (3) scalenohedral calcites, and (4) variously sized granular calcite cements. In addition, some modifications of RFC cements as well as drusy mosaic calcite occur.

Marine phreatic isopachous cement followed by void-filling granular cement occurs only locally. Some isopachous cements continue growing as RFC . Additional diagenetic features are microspar as well as vadose silt and hematite seams (occurring as dust on smooth surfaces of RFC and as internal sediment).

6.1 Radiaxial-fibrous calcite (RFC)

RFC represents the volumetrically most abundant cement type in the samples studied and is characterized by large cloudy (inclusion-rich) crystals with curved boundaries and twin lamellae, oriented perpendicular to subperpendicular to the substrate. We have made no distinction between 'radiaxial-fibrous calcite' (BATHURST, 1959), 'fascicular-optic calcite' (KENDALL, 1977), 'radial-fibrous calcite' (DAVIES, 1977; MAZZULLO, 1980) and 'radial-radiaxial calcite' (PREZBINDOWSKI, 1985) and use RFC in the sense of KENDALL (1985) as a term for 'a variety of calcite cements composed of crystals with undulose extinction and abundant inclusions that make them cloudy or turbid'.

6.1.1 Criteria and original mineralogy

These cements exhibit distinct growth zones which differ in crystal size and morphology (pl. 1/5–6, pl. 3/5–6, pl. 4/1). The zones are separated by dirty seams (pl. 1/5–6, pl. 4/1) or by a thin cover of poorly sorted carbonate silt with angular crystal fragments (pl. 2/5–6, pl. 3/1–2, pl. 4/4–6) resembling 'vadose silt' (DUNHAM, 1969). Some RFC cements are characterized by

crystals exhibiting more laterally broadened or even blocky habits (pl. 1/3, pl. 3/3, pl. 4/2). These RFCs are commonly associated with internal sediments (crystal silt) and recrystallized micritic matrix (microspar).

The radiaxial-fibrous calcite cement is concentrated in limestones rich in mollusk shells and in boundstones, exhibiting abundant interparticle and biomoldic porosity. The negative correlation of RFC cement and micritic matrix (fig. 4) points to a strong circulation of marine pore waters in the grain-/rudstones of the shell beds and in the boundstones. Slightly higher amounts of peloidal matrix had no inhibiting effect on pore-water flow and the formation of RFC.

The substrate for the subnormally growing RFC crystals is formed by mollusk shells, by micrite envelopes as well as by coral and sponge fragments. The distinct association with bioclasts may point to a control of the RFC precipitation by organic matter (cf. BOROWITZKA, 1989). Similar associations were observed by KOCH & OGORELEC (1990) and GRÖTSCH et al. (1994).

Radiaxial-fibrous calcites have been interpreted differently with regard to the environments of their formation (meteoric: SCHNEIDER, 1977; marine: KREBS, 1969; KENDALL & TUCKER, 1973) and their original mineralogy. They have been interpreted as a) neomorphic replacement products of marine precursor aragonite cements (KENDALL & TUCKER, 1973; KENDALL, 1977; MAZZULLO, 1980) or precursor Mg-calcite cements (PREZBINDOWSKI, 1985; SALLER, 1986), and b) primary calcite or Mg-calcite cements formed as composite crystals within a marine phreatic environment (KENDALL 1985, SATTERLEY et al. 1994). The criteria observed in the Steinplatte samples support the latter interpretation:

a) The individual zones of the well-preserved RFC exhibit smooth growth surfaces (pl. 1/5–6, pl. 2/5–6, pl. 4/4–6). The optical orientation of the c-axes is normal to subnormal to the substrate. Crystals of subsequent zones are equally oriented and use former crystals as nucleation sites (except if nucleation is inhibited by a silt cover). The relatively uniform growth of the crystals and the smooth growth boundary point to originally Mg-calcite crystals. A replacement of aragonite precursor crystals should result in irregular growth surfaces.
b) A primary Mg-calcite mineralogy is also indicated by the growth of RFC on an echinoderm fragment (pl. 2/4). The trigonal scalenohedral crystal lattice of the Mg-calcite of the bioclast facilitates the growth of Mg-calcite RFC cement.
c) The formation of abundant Mg-calcite cements and the good preservation of the RFC is more reasonable in the primary open pore systems of an 'active marine phreatic zone' (LONGMAN, 1980). Stagnant conditions which would facilitate preservation and slow alteration of precursor aragonite are difficult to postulate owing to the slope setting of the Steinplatte sections.
d) The good preservation of the RFC can be better explained assuming a primary Mg-calcite mineralogy, which enhances the possibility of microstructural preservation of Mg-calcites during alteration within specific ultra-environments (OTI & MÜLLER, 1985).

In conclusion, four essential factors trigger the formation of the radiaxial-fibrous calcite cements of the Steinplatte mound facies:

- the existence of sufficient pore space provided by interparticle and biomoldic pores,
- high flow rates of marine waters,
- the absence of micrite matrix acting as a permeability barrier,
- appropriate substrates (bioclasts) favoring high nucleation rates.

6.1.2 Variations of RFC cements

Some morphological variations of RFC cement seem to be caused by early disturbance of

crystal growth. Stubby variations of RFC (pl. 3/3), locally also a blocky variation (pl. 4/2), occur together with high amounts of silty internal sediment. The occurrence of crystal silt and the formation of dolomite and dedolomite within this internal sediment (pl. 3/3-4) point to the alteration of marine pore waters, to more brackish conditions or to meteoric influx. Low Mg/Ca ratio of that pore water would favour formation of stubby crystals rather than fibrous elongated crystals (FOLK, 1974) and facilitate recrystallization, resulting in the formation of blocky crystals.

PREZBINDOWSKI (1985, p. 247) reports common intervals of sediment between individual cement layers composed of radial-radiaxial calcite cements, very similar to the sediment deposited after the formation of the stubby variation of the Steinplatte RFC (pl. 3/3). PREZBINDOWSKI states that the occurrence of criteria pointing to a meteoric-water diagenesis prior to the formation of RFC cements does not necessarily argue against a marine origin of the latter if a shelf-edge position with sporadic exposures above wave base can be assumed.

6.2 Syntaxial overgrowth

Syntaxial calcite overgrowth cement (rim cement, BATHURST, 1958), generally growing on echinoderm fragments (cf. LUCIA, 1962; EVAMY & SHEARMAN, 1965, 1969), is commonly regarded as an indication of formation within the meteoric phreatic environment (LONGMAN, 1980). This interpretation was underscored by WALKDEN & BERRY (1984) who recognized a characteristic 'solution corona' within the micrite surrounding the echinoderm fragment, filled with syntaxial overgrowth. This cement occurs commonly in grainstones. It is zoned. The first inclusion-rich zones may have precipitated in a near-surface marine, meteoric or mixing-zone environment whereas the following clear overgrowth cement is regarded as being formed within the burial environment (TUCKER & WRIGHT, 1990).

In the Steinplatte samples, syntaxial overgrowth occurs only on echinoderm surfaces without micritic coatings. Clean surfaces are necessary for the nucleation of crystals growing in optical continuity. Syntaxial cements are absent on echinoderm fragments with thicker micrite crusts and on those embedded within dense micrite hindering the access of water (pl. 2/3).

Overgrowth on echinoderm fragments occurs in specific intervals, characterized by the association of the following diagenetic criteria:

1) The matrix of pack- and wackestones exhibiting syntaxial echinoderm overgrowth is commonly recrystallized to microspar (pl. 4/2–3).
2) Vugs and abundant biomolds are common within the micritic matrix (fig. 4).
3) Corals and sponges, indicative of a normal marine environment, are rare or absent.
4) Radiaxial-fibrous calcite cements are rare or absent, too.
5) Vadose (?) silt occurs in the intervals which exhibit common echinoderm overgrowth.
6) Coexisting RFC cements in packstones are characterized by first generations composed of short and bladed crystals, probably indicating an end to crystal growth (pl. 1/3, pl. 3/3, pl. 4/2).
7) RFC crystals (pl. 4/3) show clear scalenohedral terminations.
8) Gravitational dissolution areas within the matrix filled by cement also occur (pl. 1/1–2).

These criteria point to a non-marine or altered chemistry of primarily marine pore waters. The association of the criteria listed above indicates meteoric influence.

6.3 Scalenohedral calcites

Scalenohedral calcite crystals (dog tooth, BATHURST, 1959) occur commonly together with crystal silt (pl. 4/3), microsparite and syn-

taxial echinoderm overgrowth (cf. fig. 4). Locally, the terminations of RFC cement crystals exhibit the beginning of an imperfect growth of clear scalenohedral crystals. Scalenohedral crystals as well as blocky calcites are ascribed to a meteoric origin with a low Mg/Ca ratio favoring a lateral growth (b-axis) of calcite crystals (FOLK, 1974).

The scalenohedral cement crystals, therefore, may mark regressive events within the section studied. Some of the scalenohedrons, however, could be the result of later meteoric influences during the Liassic, subsequent to fracturing and infill of reddish Liassic sediments and the formation of microspar (cf. STANTON & FLÜGEL, 1989), which differ significantly from the Upper Rhaetian microsparite.

6.4 Microspar

Microspar is commonly explained as an early diagenetic, meteorically controlled recrystallization product of micritic matrix affected by aggrading neomorphism (FOLK 1962, 1974; BATHURST 1971). In our material, especially in samples from the lower part of unit-I, microspar is characteristically associated with features indicating an early diagenetic meteoric influence: Syntaxial echinoderm overgrowth, scalenohedral calcites, crystal silt, dissolution vugs and molds of particles or matrix as well as recrystallized former isopachous RFC cement.

6.5 Vadose silt

Coarse, poorly sorted crystal silt corresponding to 'vadose silt' (DUNHAM, 1969; AISSAOUI & PURSER, 1983) exhibits a characteristic distribution pattern in some parts of the sections (cf. fig. 4; pl. 1/3, pl. 3/1–2, pl. 3/3, pl. 4/2)) and occurs together with scalenohedral calcites and echinoderm overgrowth.

6.6 Hematite seams and reddish internal sediment

These features, observed in a few samples of the three sections, are most common in section C. Generally, thin hematite seams occur together with RFC cement. The hematite may indicate a short-term interruption of crystal growth or the presence of hematite dust in pore waters causing the growth of impure RFC cements (pl. 4/4–6). This can be compared with the 'denser zones of inclusions' as described by KENDALL (1985). In addition, silty reddish hematite dust covers RFC crystal surfaces. Thicker covers interrupt the growth of crystals (pl. 4/4–6).

Some of the samples exhibiting hematite seams are located near boundaries of depositional units and can be followed from section to section, indicating lower sedimentation rates at the boundaries, enabling the hematite in the RFC cement crusts to be enriched. An explanation of the hematite as being due to late infiltrations along microfractures is not possible because the RFC cements showing hematite covers are overlain by Rhaetian marine sediments.

6.7 Additional cement types

Granular cement, drusy mosaic cement as well as relics of isopachous marine-phreatic cement are less frequent in the sections studied than radiaxial-fibrous cements. They have not been studied in detail.

The nearly exclusive occurrence of equant and heterogranular cement in relic pore spaces in intervals of the sections exhibiting abundant solution porosity (mold and vugs) point to an early meteoric phreatic origin of these cements. Clear granular cement, however, occurs also in tectonic fractures cutting through particles and earlier formed cements.

Drusy cement, formed subsequent to radiaxial-fibrous or other cements occurs only locally

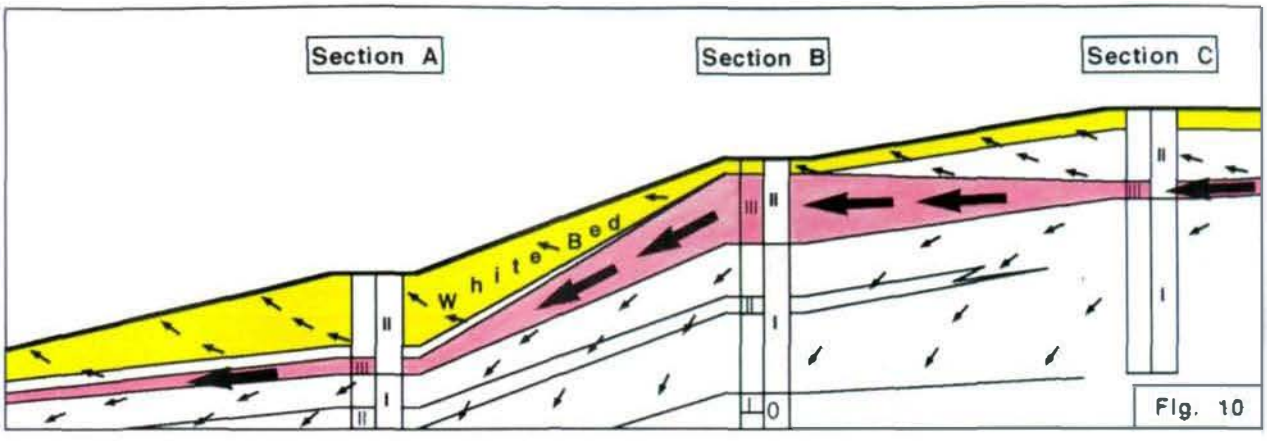

Fig. 10: Sketch of the hydrological system acting subsequent to the deposition of the 'White bed' and influencing the depositional units I and II. An early meteoric influx, using the permeable 'White bed' as conduit caused recrystallization to microspar in the underlying beds and local formation of vugs which were later filled by granular cement. In the 'White bed' primary aragonitic grains are dissolved. Subsequent influx of marine pore waters resulted in the formation of RFC on mollusk shells and boundstone substrates. Arrows indicate pore water flux.

in the center of larger pores. The formation of drusy cement was not controlled by specific porosity types.

Isopachous marine-phreatic cement seams consisting of normally and subnormally oriented relictic blades and needles are rare and restricted to primary interparticle pores. The thickness of the seams varies between 50 and 100 µm. The crystals of the seams border only locally on granular cement. Locally they continue their growth as radiaxial-fibrous cements.

7. Discussion

The 'mound facies' of the Steinplatte comprises at least three aggradational cycles consisting of different rock types documented by the depositional units 0, I, II, III and IV. Each cycle is characterized by lateral variations in thickness and in composition (matrix, grains, primary porosity). These variations caused differences in conduits of pore waters, whose composition changed through time (fig. 9-11).

A main break in the sedimentary history is marked by the top of the 'White Bed' separating unit-II and unit-III. Another, less distinct break occurs between unit-III and unit-IV. The overlying unit-IV continues into the 'Capping beds' whose diagenesis was studied by MAZZULLO et al. (1990).

Regarding the frequency of matrix, grains, porosity types and common cement types, some marked interrelations are obvious.

The first aggradational cycle (units-0, -I and -II; fig. 10) consists of *a lower part* (units-0 and -I) characterized by large amounts of micritic matrix, and consequently, low primary interparticle porosity. Only shell bed II (packstones and grainstones), intercalated within the predominantly micritic sediment indicates the local existence of some higher porosity. The distribution of RFC cements is controlled by the spatial distribution of shell beds and/or of boundstones.

The *middle part* of the first cycle is represented by shell bed III. The formation of abundant RFC was controlled by high interparticle and biomoldic porosity related to the high number of bioclastic grains.

The *upper part* of the cycle corresponds to the 'White bed', best developed in section A. It is characterized by high amounts of micritic and peloidal matrix as well as fine bioclastic debris. The primary framework of boundstones (sec-

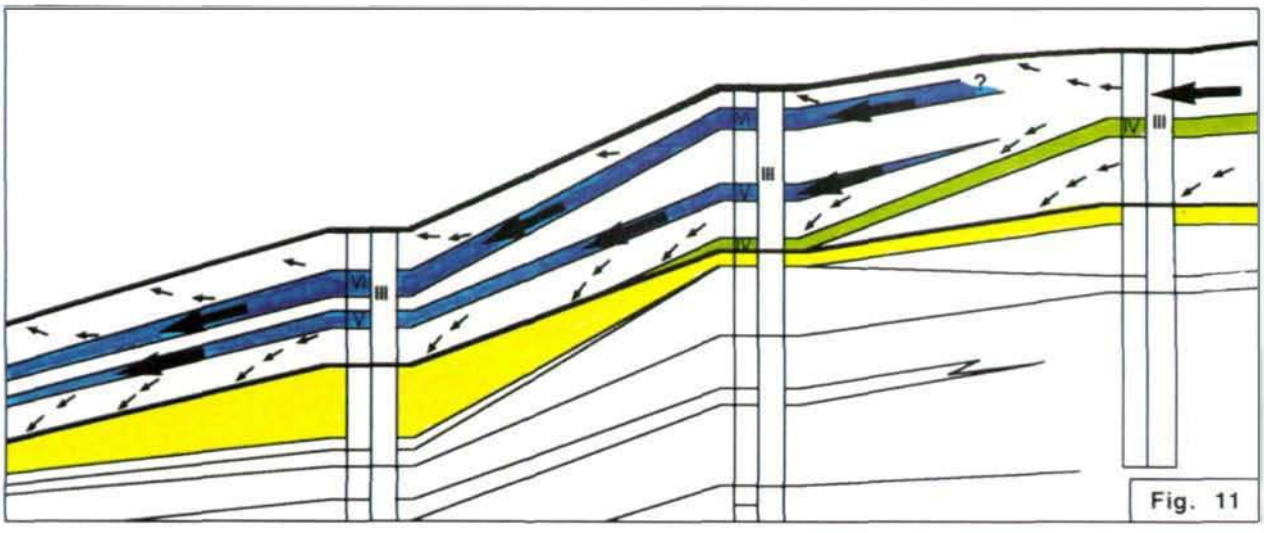

Fig. 11: Sketch of the hydrological system acting subsequent to the deposition of shell bed VI and influencing predominantly the sediments of the second aggradational cycle. Main conduits for meteoric and altered marine waters are the shell beds V and VI. Arrows indicate pore water flux.

tion C) rendered appropriate substrates for the formation of RFC.

Many RFC cements occur in molds formed by dissolution of mollusk shells and now preserved as micrite envelopes. The formation of RFC on micrite envelopes points to a corresponding mineralogy (Mg-calcite) of RFC and the internal cement fillings of microborings causing the micrite envelopes (ALEXANDERSSON, 1972; WINLAND, 1971; KENDALL, 1985).

The vertical and lateral alternation of sediment types and the distributional patterns of the diagenetic criteria are best explained by the assumption of a 'layer-cake' shaped internal structure of the first aggradation cycle allowing changes in the flow of pore waters of varying composition and in the formation of different carbonate cements.

The dissolution of primary aragonitic bioclasts and the Mg-calcite to calcite transformation within the micrite envelopes of unit-III is explained by an early diagenetic influx of meteoric waters subsequent to the deposition of the 'White Bed' and using shell bed III as conduit during the maximum of a regression period. Simultaneously, meteoric pore waters penetrated the underlying sediments of unit-I and influenced the micritic matrix of the 'White Bed' as indicated by the formation of microspar and many vugs caused by local dissolution of micrite and the enlargement of molds. The abundant occurrence of syntaxial overgrowth cements, vadose silt within many molds and vugs as well as dedolomite in section B (just below the top of the 'White Bed'), is ascribed to the same process. The formation of dedolomite could be caused by near-surface pore waters rich in CO_2 and affecting dolomite originating from the recrystallization of a Mg-calcite micrite matrix (RICHTER, 1988).

Subsequent growth of RFC cements (on calcite and Mg-calcite substrates) during marine conditions was interrupted as indicated by thin covers of vadose silt on the first RFC generations and covers of hematite dust. These interruptions could be caused by influx of silt from more shallow areas (section C) and from subaerially exposed areas. As shown by AISSAOUI & PURSER (1983), vadose silt can be deposited several meters below the depositional interface.

The hydrological system affecting the **second aggradational cycle** may have been slightly different from that of the hydrological system described above because of the more isolated position of the shell beds sandwiched between micritic beds and providing major conduits.

Sediments of unit-III were deposited on a smooth relief formed by shell bed IV (fig. 11). Dissolution of aragonitic grains, microspar, vugs and granular cement indicate meteoric influx at the top of shell bed IV invading the system from the east (section C) . The top of the second aggradational cycle is marked by the occurrence of dog tooth cement and RFC cements exhibiting scalenohedral terminations, pointing again to repeated meteoric overprints.

The **third aggradational cycle** includes shell bed VII as well as the 'capping beds' of the 'coral garden' studied by MAZZULLO et al. (1990) who documented different generations of RFC cement exhibiting growth interruptions. RFC cement occurs in isopachous laminated crusts in dissolution cavities and biomolds, associated with internal sediments.

Although the cement types described by MAZZULLO et al. also occur in the 'mound facies' studied by us, it seems premature to attribute the diagenetic processes of the capping facies and the mound facies to the same general pattern. MAZZULLO et al. have only studied samples from the uppermost 10 to 20 meters of the Steinplatte limestone, which comprises a total thickness of about 150 meter.

Marked differences between our study and the results of MAZZULLO et al. concern the size of dissolution cavities. Molds and vugs observed in the 'mound facies' are within a millimeter scale. In contrast, the cavities described from the uppermost coral limestone of the capping facies of the Steinplatte just below the Triassic/Liassic boundary surface have dimensions of 30–40 cm and more. Similar large-scaled dissolution cavities, described by SATTERLEY et al. (1994) from the Oberrhätkalk near the Triassic/Liassic boundary of the Wilde Kirche (Karwendel Mountains) correspond to karst features. Using the data discussed by SATTERLEY et al., the time needed for the formation of the small-scaled vugs and molds of the 'mound facies' was relatively short as compared with the long-term karstification of the Wilde Kirche example.

Other differences concern the interrelations between specific rock types and the abundance of molds and vugs. In contrast to the small vugs of the Steinplatte 'mound facies' the large cavities described by MAZZULLO et al. (1990) and SATTERLEY et al. (1994) are irregularly distributed throughout the rocks and exhibit no preference with regard to particular lithofacies types or a specific stratigraphic position.

Karstification may cause a deep-reaching recrystallization reaching down to 40–60 meter below the upper karst surface (SATTERLEY et al., 1994). This corresponds to patterns observed in the 'mound facies': Regarding the top of the 'White bed' as omission surface, indications of meteoric diagenesis (vugs and syntaxial echinoderm overgrowth) occur just about 40 m below shell bed III which probably acted as meteoric conduit (fig. 4). Similar downward effects occur in the two other aggradational cycles.

Similarities between the cements of the 'capping beds' studied by MAZZULLO et al. (1990) and of the 'mound facies' concern the types of the radiaxial-fibrous cements as well as the growth interruptions of these cements marked by the separation of RFC generations by reddish internal sediment and by hematite-stained microdissolution surfaces which truncate the first RFC generation. This indicates, that the early RFC generations have suffered more recrystallization stages as compared with the latter ones. Nevertheless, all recrystallization textures are well-preserved. This corresponds to the first alteration of FC cement in the Wilde Kirche (SATTERLEY et al., 1994).

Despite these similarities, the controls on the formation of the RFC cements were different for

the 'capping facies' and the 'mound facies'. The distributional pattern of RFC cements of the mound facies depends on variations of primary matrix contents, early porosity pathways, and permeability within a sedimentary layer-cake structure which caused different hydrological systems at different times.

8. Conclusions

1) The 'mound facies' exposed in the Steinplatte cliff sections comprises at least three aggradational cycles which were interrupted by regressive phases as documented by omission surfaces and disconformities. Vertical as well as lateral facies differences within these cycles resulted in the formation of complex hydrological systems acting as flow pathways for marine and/or meteoric or altered pore waters.
2) The flow pathways were intensified by the effect of repeated early meteoric influx causing dissolution of mineralogically instable bioclasts (predominantly mollusks). Increasing access of pore waters resulted in the formation of molds and vugs and the recrystallization of great parts of the rocks above and below the beds which act as pore water conduits. This process took place within each aggradational cycle pointing to synsedimentary changes in pore water chemistry.
3) Subsequent repeated influx of marine pore waters resulted in the abundant formation of radiaxial-fibrous calcite cements whose growth was strongly substrate-controlled. Interruptions of cement growth by reddish silt and vadose silt point to karstification of adjacent platform areas.
4) The diagenesis of the Steinplatte differs from that of platform carbonates characterized by continuous marine cementation. Due to the strong vertical and lateral facies differentiation diagenesis corresponds to an interplay of meteoric and marine phases.
5) Intervals exhibiting moldic and vuggy porosity are not caused by Triassic/Jurassic (or recent) karstification but are the result of a downslope influx of meteoric waters within the sediment bodies.
6) The 'mound facies' of the Steinplatte is an example of a complex cementation pattern controlled by (1) the spatial distribution of primary facies criteria (matrix, grains, porosity types), (2) sedimentation within aggradational cycles on a ramp, causing variations of the hydrological systems in time, and (3) local substrate control favoring the predominant precipitation of radiaxial-fibrous calcite cement.

Acknowledgements

The study is part of the project 'Evolution of Reefs', funded by the Deutsche Forschungsgemeinschaft.The authors would like to thank Robert J. Stanton (Texas A & M University, College Station) for stimulating discussions in the field, and the technical staff of the Erlangen Institute of Paleontology for assistance in preparing samples and microphotographs.

References

AIGNER, T. (1982): Calcareous tempestites: storm-dominated stratification in Upper Muschelkalk limestones (Triassic, SW-Germany). – In: EINSELE, G. & SEILACHER, A. (eds.): Cyclic and event stratification, 180–198, Berlin (Springer).

AIGNER, T. (1986): Storm depositional systems. Dynamic stratigraphy in modern and ancient shallow-marine sequences. – Lecture Notes in Earth Sciences, **3**, 174 p., 83 figs., Berlin (Springer).

AISSAOUI, D.M. & PURSER, B. (1983): Nature of origins of internal sediments in Jurassic limestones of Burgundy (France) and Fnoud (Algeria). – Sedimentology, **30**, 273–283, Oxford.

ALEXANDERSSON, T. (1972): Intragranular growth of marine aragonite and Mg-calcite: evidence of precipitation from supersaturated sea water. – J. Sed. Petrol., **42**, 441–460, Tulsa.

BATHURST, R.G.C. (1958): Diagenetic fabrics in some British Dinantian limestones. – Liverpool Manchester Geol. J., **2,** 11–36, Liverpool.

BATHURST, R.G.C. (1959): The cavernous structure of some Mississipian stromatactis reefs in Lancashire, England. - J. Geol., 67, 506–521, Liverpool.

BATHURST, R.G.C. (1971): Carbonate sediments and their diagenesis – Developments in Sedimentol., **12**, 620 p., London (Elsevier) .

BOROWITZKA, M.A. (1989): Carbonate calcification in algae - Initiation and control. – In MANN, S., WEBB, J. & WILLIAMS, R.P. (eds.): Biomineralization, 63–94, Cambridge (VCH Publishers).

BRICKER, O.P. (ed.) (1971): Carbonate Cements. – Johns Hopkins Univ. Stud. Geol., **19**, 376 pp., Baltimore.

CHOQUETTE, P.W. & PRAY, L.C. (1970): Geologic nomenclature and classification of porosity in sedimentary carbonates. – Amer. Ass. Petrol. Geol. Bull., **54**, 207–250, Tulsa.

DAVIES, G. R. (1977): Former magnesium in calcite and aragonite submarine cements in Upper Palaeozoic reefs in the Canadian Arctic: a summary. – Geology, **5**, 11–15, Boulder.

DUNHAM, R.J. (1962): Classification of carbonate rocks according to depositional texture. – In HAM, W.E. (ed): Classification of carbonate rocks. – Amer. Assoc. Petrol. Geol. Mem., **1**, 108–121, Tulsa.

DUNHAM, R. (1969): Early vadose silt in Townsend Mound (reef), New Mexico. – In: FRIEDMAN, G.M. (ed.): Depositional environments in carbonate rocks. – SEPM Spec. Publ., **14**, 139–181, Tulsa.

EVAMY, B.D. & SHEARMAN, D.J. (1965): The development of overgrowth from echinoderm fragments in limestones. – Sedimentology, **5**, 211–233, Oxford.

EVAMY, B.D. & SHEARMAN, D.J. (1969): Early stages in development of overgrowth on echinoderm fragments in limestones. – Sedimentology, **12**, 317–322, Oxford.

FOLK, R. L. (1962): Spectral subdivision of limestone types. – In HAM, W.E. (ed): Classification of carbonate rocks. – Amer. Assoc. Petrol. Geol. Mem., **1**, 62–84, Tulsa.

FOLK, R.L. (1974):The natural history of crystalline calcium carbonate: Effect of magnesium content and salinity. – J. Sed. Petrol., **44**, 40–53, Tulsa.

FÜRSICH, F. T. (1978): The influence of faunal condensation and mixing on the preservation of fossil benthic communities. – Lethaia, **11**, 243–250, 7 figs., Oslo.

GOLEBIOWSKI, R. (1991): Becken und Riffe der alpinen Obertrias. Lithostratigraphie und Biofazies der Kössener Formation. – Exkursionen im Jungpaläozoikum und Mesozoikum Österreichs, 79–119, Wien (Österr. Paläont. Ges.).

GRÖTSCH, J., KOCH, R. & BUSER, S. (1994): Fazies, Gildenstruktur und Diagenese des nördlichen Randes der Dinarischen Karbonatplattform (Barrême-Apt, W-Slowenien). – Abh. Geol. B.-A., **50**, 125–153, Wien.

HAHN, F.F. (1910): Die Geologie der Kammerker-Sontagshorngruppe. 1. Teil. – Jb. Geol. Reichsanstalt, **60**, 311–420, pls. 16–17, 20 figs., Wien.

HARRIS, P. M., KENDALL, C. G. & LERCHE, J. (1985): Carbonate cementation: a brief review. – In: SCHNEIDERMANN, N., HARRIS, P. M. (eds.): Carbonate cements. – Soc. Econ. Paleont. Min. Spec. Publ., **36**, 79–95, Tulsa.

KENDALL, A.C. (1977): Fascicular-optic calcite: A replacement of bundled acicular carbonate cements. – J. Sed. Petrol., **47**, 1056–1062, Tulsa.

KENDALL, A.C. (1985): Radiaxial fibrous calcite: A reappraisal. – In: SCHNEIDERMANN, N. & HARRIS, P.M. (eds.): Carbonate Cements. Soc. Econ. Paleont. Min. Spec. Publ., **36**, 59–77, Tulsa.

KENDALL, A.C. & TUCKER, M.E. (1973): Radiaxial fibrous calcite: a replacement after acicular carbonate. – Sedimentology, **20**, 365–389, Amsterdam.

KIDWELL, S.M. & AIGNER, T. (1985): Sedimentary dynamics of complex shell beds: implications for ecologic and evolutionary patterns. – In: BAYER, U. & SEILACHER, A. (eds.): Sedimentary and evolutionary cycles. – Lecture Notes in Earth Sciences, **1**, 382–395, 4 figs., Stuttgart (Schweizerbart).

KIDWELL, S.M., FÜRSICH, F.T. & AIGNER, T. (1986): Conceptual framework for the analysis and classification of fossil concentrations. – Palaios, **1**, 228–238, 5 figs., Ann Arbor.

KOCH, R. & OGORELEC, B. (1990): Biogenic Constituents, cement types and sedimentary fabrics. – In: HELING, D., ROTHE, P., FÖRSTNER, U. & STOFFERS, P. (eds.): Sediments and Environmental Geochemistry, 95–23; Springer (Berlin, Heidelberg, New York).

KREBS, W. (1969): Early void-filling cementation in Devonian fore-reef limestones (Germany). – Sedimentology, **12**, 279–299, Amsterdam.

LIGHTY, R.G. (1985): Preservation of internal reef porosity and diagenetic sealing of submerged early Holo-

cene barrier reef, southeastern Florida shelf. – Soc. Econ. Paleont. Min. Spec. Publ., **36**, 123–151, 45 figs., Tulsa.

LOBITZER, H. (1980): The Steinplatte carbonate platform/basin-complex (Norian/'Rhaetian', Northern Calcareous Alps. – In: BOSELLINI, A., LOBITZER, H., BRANDNER, R., RESCH, W. & CASTELLARIN, A.: The complex basins of the Calcareous Alps and paleomargins. – Abh. Geol. B.-A., **34**, 287–325, 23 figs., Wien

LONGMAN, M. W. (1980): Carbonate diagenetic textures from near-surface diagenetic environments. – Amer. Ass. Petrol. Geol. Bull., **63**, 461–487, Tulsa.

LUCIA, F.J. (1962): Diagenesis of a crinoidal sediment.- J. Sed. Petrol., **32**, 848–865, Tulsa.

MARSHALL, J.F. (1983): Submarine cementation in a high-energy platform reef: One Tree Reef, southern Great Barrier Reef. – J. Sed. Petrol., **53**, 1133–1149, Tulsa.

MARSHALL, J.F. (1986): Regional distribution of submarine cements within an epicontinental reef system: Central Great Barrier Reef, Australia. – In: SCHROEDER, J.H. & PURSER, B.H. (eds.): Reef diagenesis, 8–26, 9 figs., Berlin (Springer)

MAZZULLO, S.J (1980): Calcite pseudospar replacive of marine acicular aragonite, and its implications for aragonite cement diagenesis. – J. Sed. Petrol., **50**, 409–422, Tulsa.

MAZZULLO, S.J., BISCHOFF, W.D. & LOBITZER, H. (1990): Diagenesis of radiaxial fibrous calcites in a subunconformity, shallow-burial setting: Upper Triassic and Liassic, Northern Calcareous Alps, Austria. – Sedimentology, **37**, 407–425, 10 figs., Oxford.

OHLEN, H.R. (1959): The Steinplatte reef complex of the Alpine Triassic (Rhaetian) of Austria. – Ph.D. thesis, Princeton University, 122 p., Princeton.

OTI, M. & MÜLLER, G. (1985): Textural and mineralogical changes in coralline algae during meteoric diagenesis: An experimental approach. – N. Jb. Miner. Abh., **151**, 163-195, Stuttgart.

PILLER, W. (1981): The Steinplatte reef complex, part of an Upper Triassic carbonate platform near Salzburg (Austria). – In: TOOMEY, D.F. (ed.): European fossil reef models. – Soc. Econ. Paleont. Min. Spec. Publ., **30**, 261-290, 23 figs., Tulsa.

PREZBINDOWSKI, D.R. (1985): Burial cementation – is it important ? A case study, Stuart City Trend, south central Texas. – In: SCHNEIDERMANN, N. & HARRIS, P.M. (eds.): Carbonate cements. – Soc. Econ. Paleont. Mineral. Spec. Publ., **36**, 241–246, Tulsa.

RICHTER, D.K. (1988): Karbonatgesteine. – In: FÜCHTBAUER, H. (ed.): Sedimente und Sedimentgesteine, 233–434, Stuttgart (Schweizerbart).

SALLER, A.H. (1986): Radiaxial calcite in Lower Miocene strata, subsurface Enewetak Atoll. – J. Sed. Petrol., **56**, 743-762, Tulsa.

SATTERLEY, A.K., MARSHALL, J.D. & FAIRCHILD, I.J. (1994): Diagenesis of an Upper Triassic reef complex, Wilde Kirche, Northern Calcareous Alps, Austria.- Sedimentology, **41**, 935–950, Oxford.

SCHÄFER, K.A. (1969): Vergleichsschaubilder zur Bestimmung des Allochemgehaltes bioklastischer Karbonatgesteine. – N. Jb. Geol. Paläont., Mh., **1969**, 173–184, Stuttgart.

SCHÄFER, P. (1979): Fazielle Entwicklung und palökologische Zonierung zweier obertriadischer Riffstrukturen in den Nördlichen Kalkalpen ('Oberrhät'-Riff-Kalke, Salzburg). – Facies, **1**, 3–24, Pls. 1–21, 46 figs., Erlangen.

SCHNEIDER, W. (1977): Diagenese devonischer Karbonatkomplexe Mitteleuropas. – Geol. Jahrb., **D 21**, 107 S., Hannover.

SIEBER, R. (1937): Neue Untersuchungen über die Stratigraphie und Ökologie der alpinen Triasfaunen. I. Die Fauna der nördlichen Rhätriffkalke.- N. Jb. Geol. Paläont., Beilage Bd., **78**, 123-188, Pl. 2-5, 5 figs., Stuttgart.

STANTON, R.J., JR. & FLÜGEL E. (1989): Problems with reef models: The late Triassic Steinplatte 'reef' (Northern Alps, Salzburg/Tyrol, Austria). – Facies, **20**, 1–138, Pl. 1–53, 33 figs., Erlangen.

STANTON, R.J., JR. & FLÜGEL, E. (1995): An accretionary distally steepened ramp at an intrashelf basin margin: an alternative explanation for the Upper Triassic Steinplatte 'reef' (Northern Calcareous Alps, Austria). – Sed. Geol. (in press)

TUCKER, M.E. & WRIGHT, V.P. (1990): Carbonate Sedimentology.- 482 pp., Oxford (Blackwell).

VORTISCH, W. (1926): Obertriadische Riffkalke und Lias in den nordöstlichen Alpen. I. – Jb. Geol. B.-A., **76**, 1–64, 1 pl., 4 figs., Wien.

WALKDEN, G.M. & BERRY, J.R. (1984): Syntaxial overgrowth in muddy crinoidal limestones: Cathodoluminescence sheds a new light on an old problem. – Sedimentology, **31**, 251–267, Oxford.

WALTER, L.M. (1985): Relative reactivity of skeletal carbonates during dissolution: Implication for diagenesis. – In: SCHNEIDERMANN, N. & HARRIS, P.M. (eds.): Carbonate Cements. – Soc. Econ. Paleomt. Min. Spec. Publ., **36**, 3–16; Tulsa.

WINLAND, H. D. (1971): Nonskeletal deposition of high-Mg calcite in the marine environment and its role in the retention of textures. – In: BRICKER, O. P. (ed.): Carbonate cements, John Hopkins Univ. Stud. Geol., **19**, 278–284, Fig. 129–131, Baltimore.

ZANKL, H. (1971): Upper Triassic carbonate facies in the Northern Limestone Alps. – In: MÜLLER, G. (ed.): Sedimentology of Central Europe, 147–185, Frankfurt (Kramer).

Authors' address:
Prof. Dr. Erik Flügel, Prof. Dr. Roman Koch, Institut für Paläontologie, Universität Erlangen-Nürnberg, Loewenichstr. 28, D–91054 Erlangen.

Manuscript submitted: February 2, 1995

Plate 1

Syntaxial echinoderm cements (Fig. 1–2), crystal silts (Fig. 3) and radiaxial-fibrous cements (Fig. 4–5). Section B. Western cliff of the Steinplatte. Oberrhätkalk.

Fig. 1: Syntaxial overgrowth on echinoderm fragments is common to abundant in the upper part of section C (shell bed VI). Many of these overgrowth cements show gravitational growth of small pendant dog-tooth like crystals into the micritic matrix (arrows) or in molds earlier formed. The boundary between these pendant crystals and the later formed coarse granular to blocky cements is indicated by double arrows. The formation of this syntaxial overgrowth corresponds to the 'solution corona' concept (WALKDEN & BERRY, 1984). The micritic matrix is recrystallized and therefore differs from the commonly dark-looking dense micritic matrix (cf. pl. 2/3). Sample 12/6. Parallel nicols. Width of the photograph 2 mm.

Fig. 2: Same sample as fig. 1. Crossed nicols. A thin micritic layer on the echinoderm fragment could not avoid syntaxial overgrowth. Width 2 mm.

Fig. 3: Silty internal sediments and molds are abundant in the uppermost part of the mound facies underlying the capping facies. Cement fringes covering the surface of the moldic pores consist of granular, laterally enlarged crystal (arrows). Sample 12/4. Parallel nicols. Width of the photograph 5 mm.

Fig. 4: Cements of shell bed VI. Radiaxial-fibrous cement consisting of large crystals surrounds lithoclasts (center top) as well as mollusk shells, echinoderm fragments (center) and coral debris (right and bottom). Dark seams separating the different zones with fibrous cements indicate an interruption of cement growth. Sample 12/7. Width of the photograph 8 mm.

Fig. 5: Radiaxial-fibrous cements, surrounding bioclastic grains of shell bed VI exhibit thicker (arrows) and thinner (double arrows) growth seams. Primary relict interparticle pores are closed by clear, predominantly granular calcite. Sample 12/7. Parallel nicols. Width of the photograph 2 mm.

Fig. 6: Detail of fig. 5 showing distinct growth seams within the radiaxial-fibrous cement. Note the differences in the thickness of the growth seams (thick, diffuse, (arrow), and fine, sharply defined (double arrow). A third generation of radiaxial-fibrous cement grows upon a distinct dirty seam and is bordered by relatively clear granular to blocky crystals toward the center of the pore (lower right corner, ; cf. pl. 1/5). Sample 12/7. Parallel nicols. Width of the photograph 2 mm.

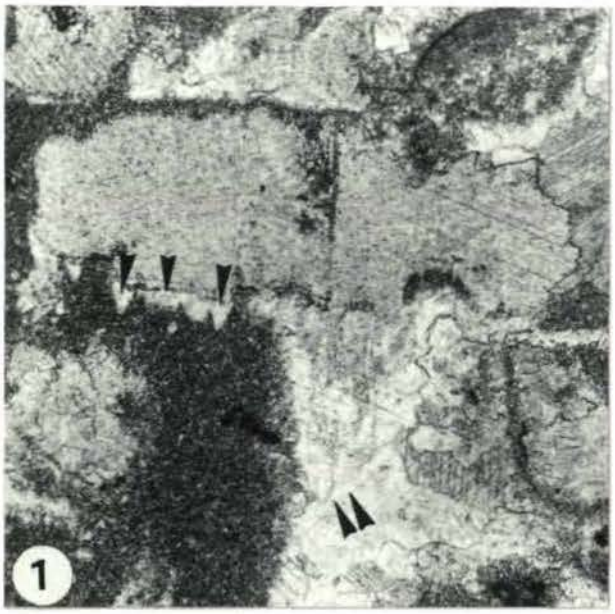
1

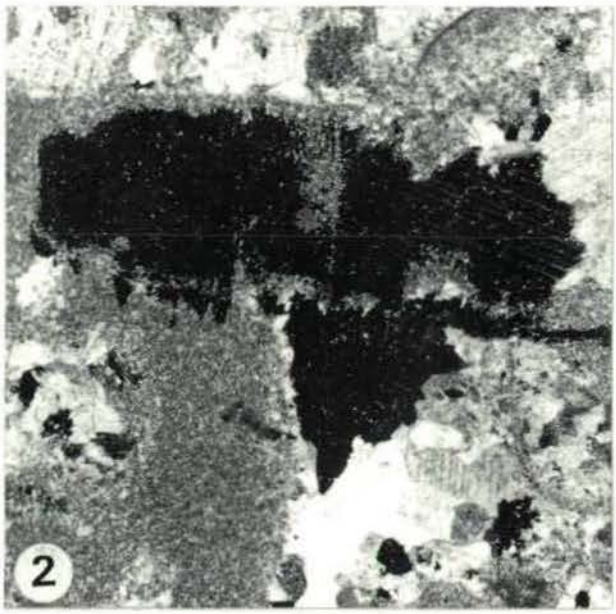
2


3

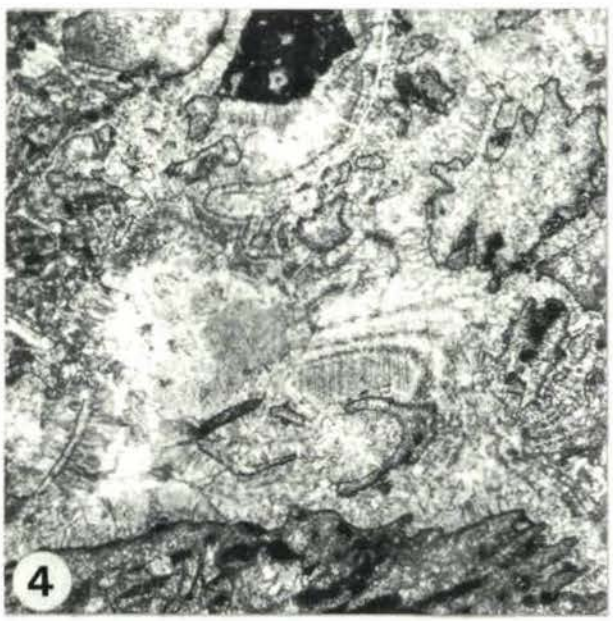
4

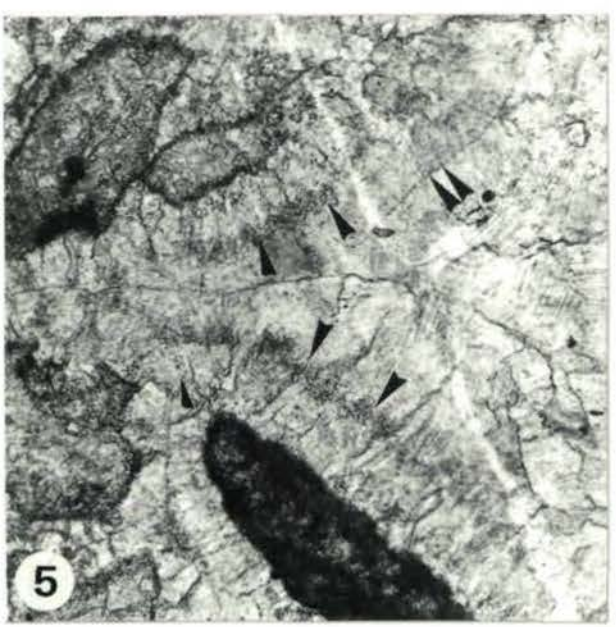
5

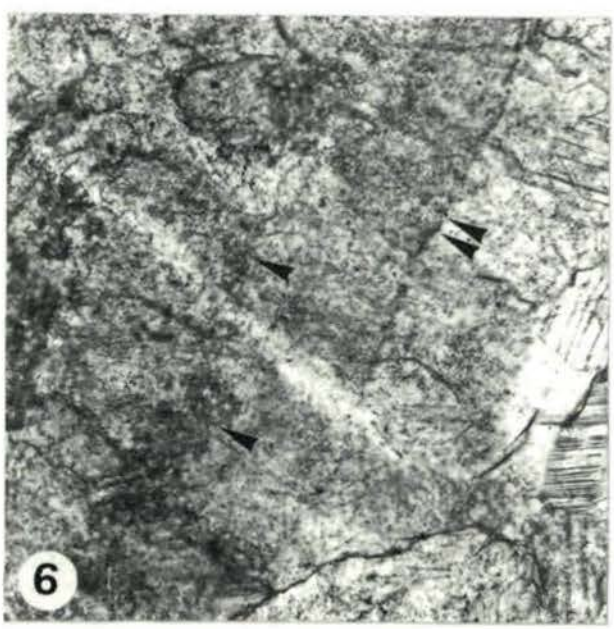
6

Plate 2

Internal sediment, micrite matrix, echinoderm overgrowth and RFC cements. Section B. Western cliff of the Steinplatte. Oberrhätkalk.

Fig. 1: Up to five generations of peloidal internal sediment within a cavity of shell bed VI. Relic pore space is filled by coarse blocky cement (top). Sample 12/8. Parallel nicols. Width of the photograph 6 mm.

Fig. 2: Detail of the internal sediment shown in Fig. 1. From bottom to top: (1) Ostracod biomicrite; ostracods floating in a pelmicritic matrix. (2) Pelsparite exhibiting peloidal cement structures (peloids surrounded by calcite). (3) Thin micrite layer; ostracods at the top. (4) Ostracod biomicrite exhibiting enrichment of ostracod shells near the top. (5) Thin micrite layer with ostracods. Note the burrowing in layer 4 and the infill from layer 5. Sample 12/8. Parallel nicols. Width of the photograph 4 mm.

Fig. 3: Biomicrite with fossil debris and a larger echinoderm fragment. The lack of syntaxial overgrowth may be due to the low porosity of the dense micrite matrix inhibiting pore water flow. The sample characterizes the micrite-rich sediment between shell bed V and shell bed VI. Sample 12/10. Parallel nicols. Width of the photograph 4 mm.

Fig. 4: Echinoderm fragment with syntaxial overgrowth, grading into radiaxial-fibrous cements surrounded by fine granular cements exhibiting undulose extinction. Sample 12/10b. Crossed nicols. Width of the photograph 2,5 mm.

Fig. 5: Radiaxial-fibrous cement within a large solution cavity at the base of depositional unit-3. A first generation of inclusion-rich cement crystals is covered by thinner (arrows) or thicker (double arrows) dark seams exhibiting granular texture and often a red color. Sample 12/14. Parallel nicols. Width of the photograph 4 mm.

Fig. 6: Same sample as Fig. 5. Crossed nicols. A second RFC generation, characterized by shorter and somewhat expanded crystals was formed (arrows) after the first generation of RFC cements and the deposition of a silty cover on the surface of the crystals. The remaining pore space is filled with coarse granular cement. Width of the photograph 4 mm.

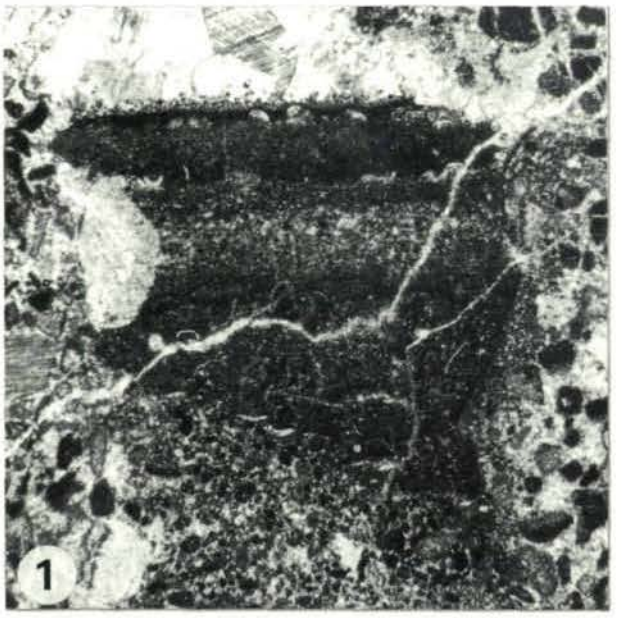
1

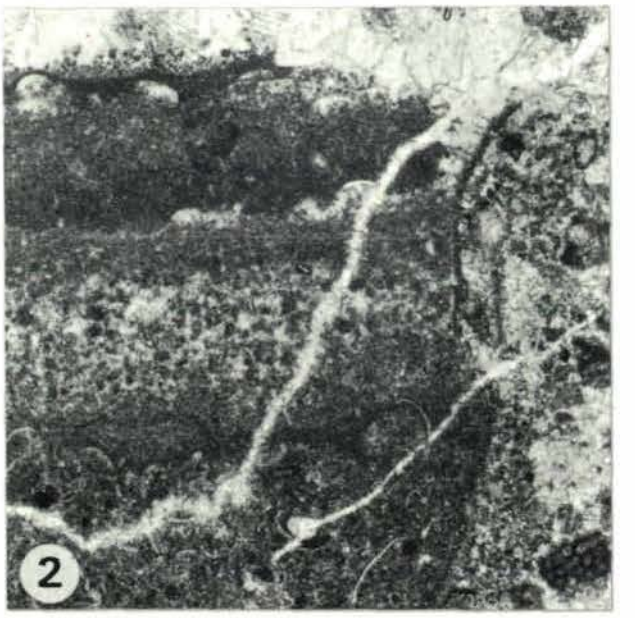
2

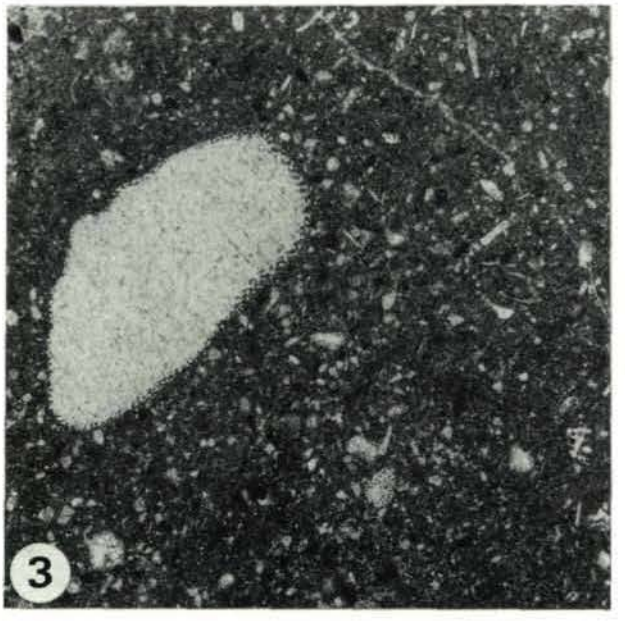
3

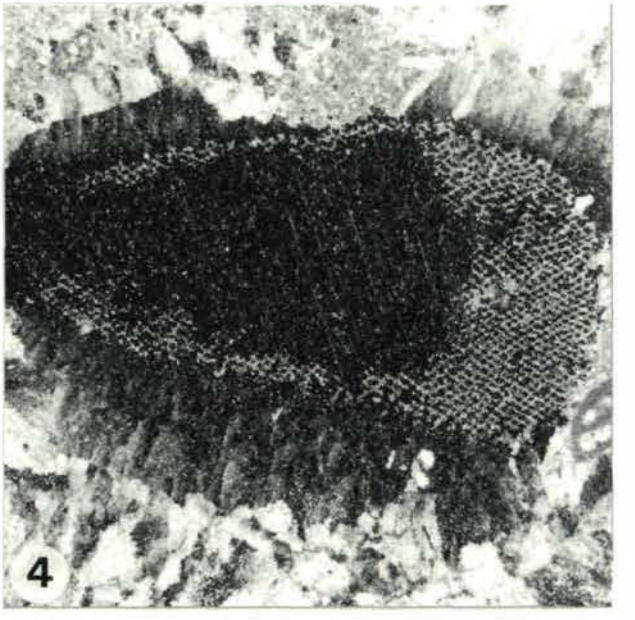
4

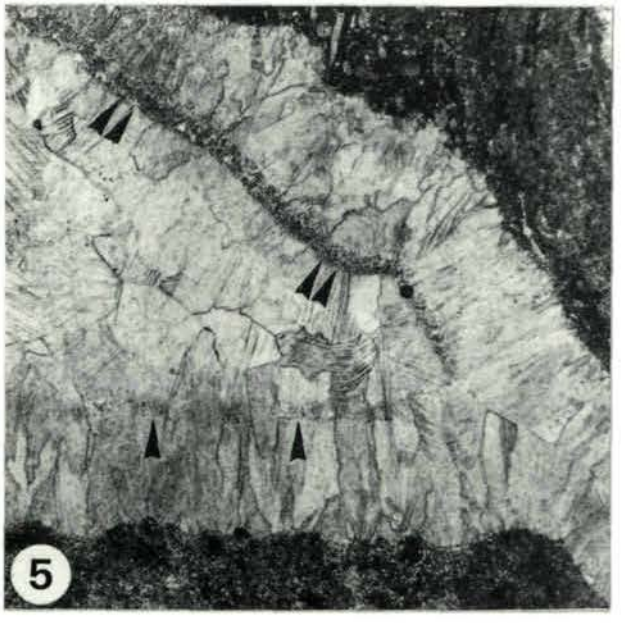
5

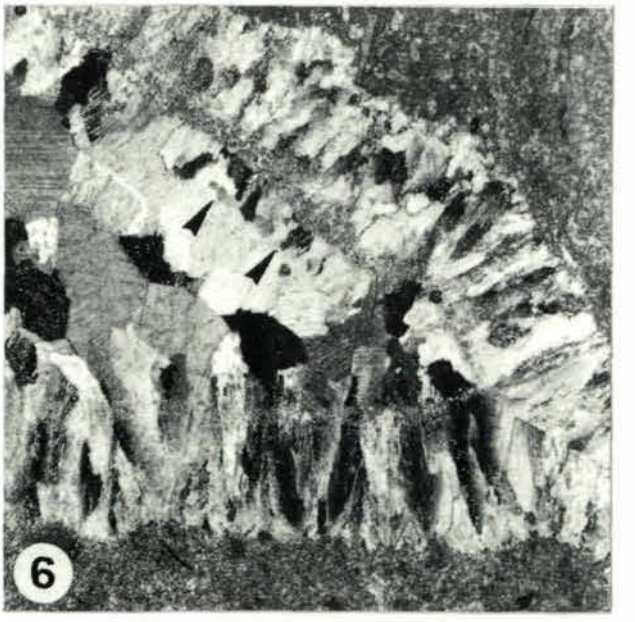
6

Plate 3

Radiaxial-fibrous cements. Section B. Western cliff of the Steinplatte. Oberrhätkalk.

Fig. 1: Detail of Pl. 2/5 and 2/6. The radiaxial-fibrous crystals of the first generation are covered by a layer of vadose silt, characterized by poorly sorted, angular crystal debris. Sample 12/14. Parallel nicols. Width of the photograph 2 mm.

Fig. 2: Same sample as Fig. 3/1. Crossed nicols. The RFC cement is covered by crystal silt including larger extended and shorter crystals. Coarse and relatively clear calcite crystals fill the center of the pore on the left. Sample 12/14. Width of the photograph 2 mm.

Fig. 3: Samples of the 'White Bed' exhibit recrystallized micritic matrix which was infilled after the formation of broad cement crystals (stubby variation of RFC), lining solution cavities. Dark spots within the recrystallized matrix are dedolomite still exhibiting the rhombohedral shape of former dolomite crystals. Sample 12/23. Parallel nicols. Width of the photograph 4 mm.

Fig. 4: Detail of Pl. 3/3 exhibiting dedolomite with well-preserved zonar relic texture of former idiomorphic dolomite rhombohedrons. Hematite (arrow), presumably formed by release of Fe^{2+} from the dolomite lattice, is oriented along former dolomite cleavage planes. Parallel nicols. Width of the photograph 1 mm.

Fig. 5: Samples from Shell Bed III exhibit the largest amounts of bioclastic grains and mollusk shells. The mollusk shells serve as nucleation sites for the growth of long radiaxial-fibrous calcite crystals. The crystals grow in the interior of a valve which is preserved as a micrite envelope. On the outside, growth of RFC was hindered by a cover of micrite. Sample 12/26. Parallel nicols. Width of the photograph 5 mm.

Fig. 6: Same sample as Fig. 3/5. Crossed nicols. Note the long RFC crystals. Width of the photograph 5 mm.

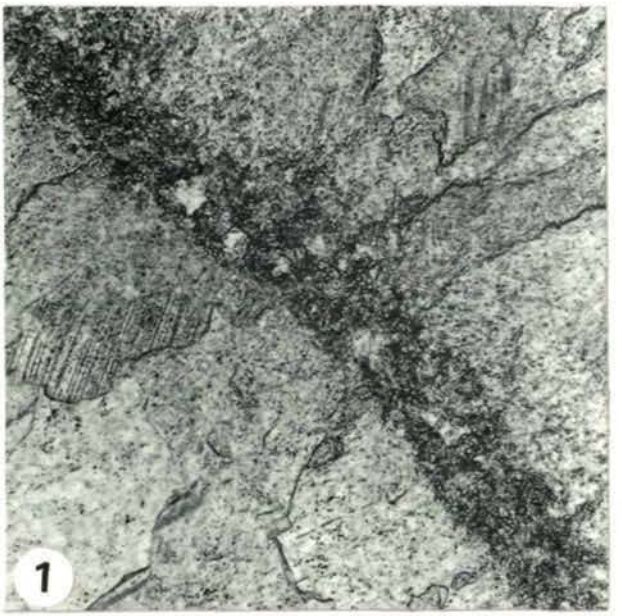
1

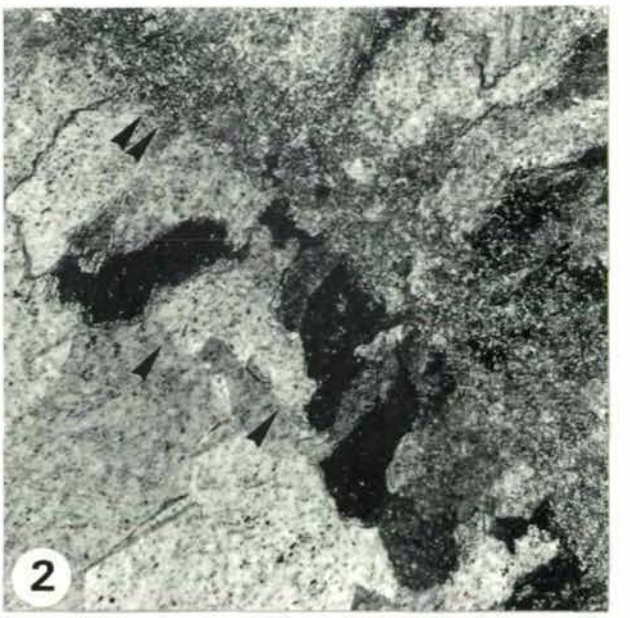
2

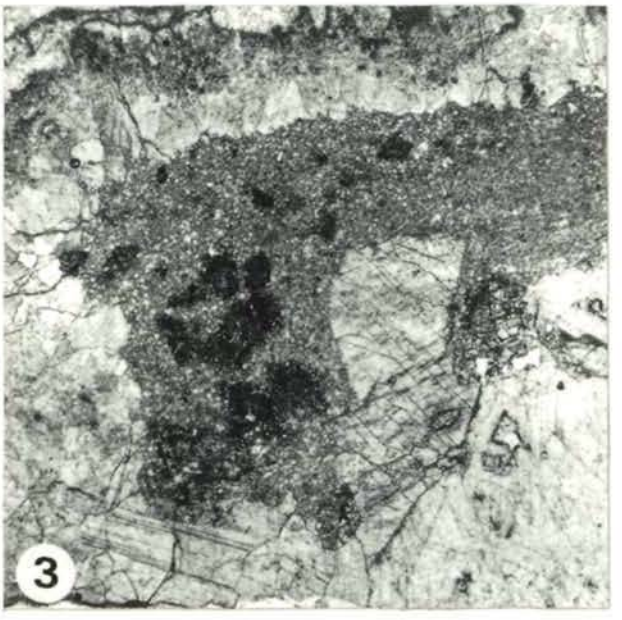
3

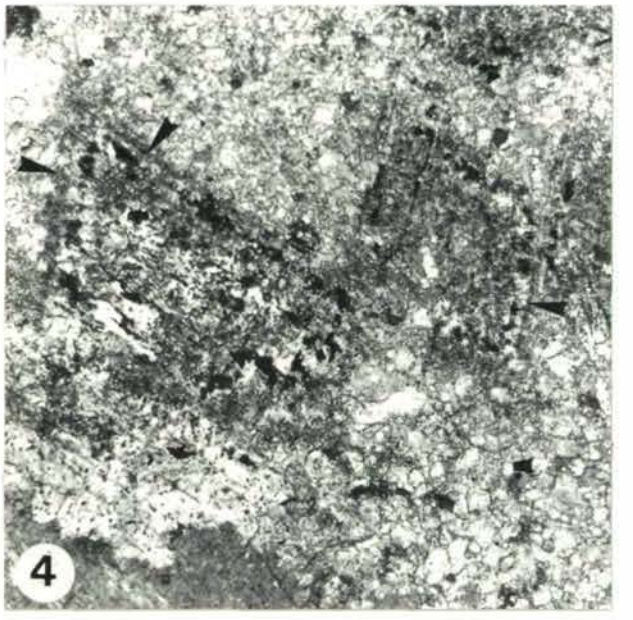
4

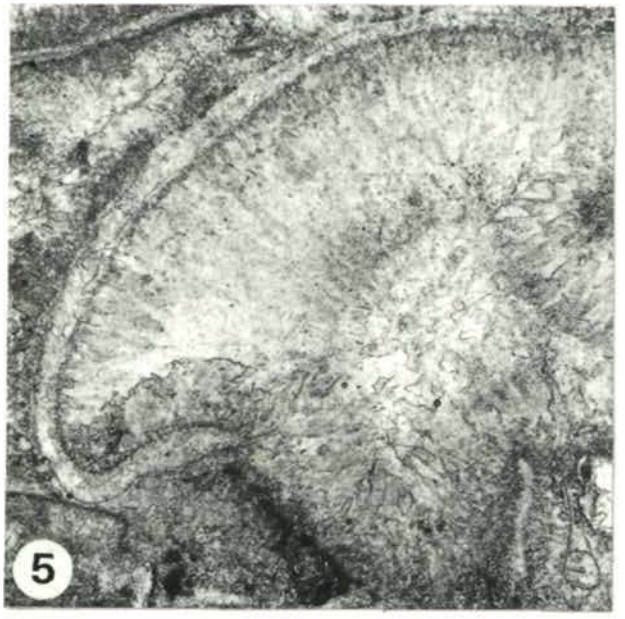
5

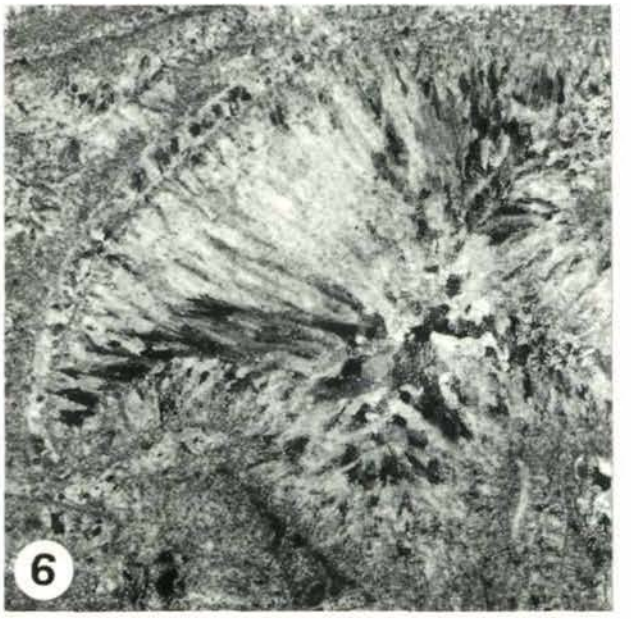
6

Plate 4

Radiaxial-fibrous cements in shell beds and solution cavities. Section B. Western cliff of the Steinplatte. Oberrhätkalk.

Fig. 1: Shell Bed III. Rudstone. Abundant pelecypod shells preserved as micrite envelopes. Growth of radiaxial-fibrous cement started upon the shells. The high primary interparticle porosity is completely occluded. Sample 12/35. Parallel nicols. Width of the photograph 5 mm.

Fig. 2: Unit-I, underlying Shell Bed III, is characterized by abundant micrite matrix, vugs and syntaxial echinoderm overgrowth. Many vugs are lined by coarse broad crystals corresponding to a stubby variation of RFC cement (arrows). The cavity is filled by a silty internal sediment. Note the differences in crystal size and color between the internal sediment and the micrite matrix (top left). Sample 12/36. Parallel nicols. Width of the photograph 2,5 mm.

Fig. 3: Solution cavity. The walls are lined with dog-tooth like granular cement (arrows). Note the difference between the silty internal sediment and the pelmicritic matrix of the rock. Depositional unit-I. Sample 12/38. Parallel nicols. Width of the photograph 4 mm.

Fig. 4: Shell Bed II is characterized by relatively large amounts of micritic matrix yielding ostracods and sessile foraminifera (bottom). Nevertheless, large solution cavities occur, filled with several generations of RFC cements. These are separated by thin or thick (arrows) silty, slightly reddish covers, which are responsible for interruptions in cement growth. Sample 12/42. Parallel nicols. Width of the photograph 5 mm.

Fig. 5: Detail of Fig. 4/4, documenting the growth boundaries within the radiaxial fibrous calcite cements. The first third of the first cement generation is covered by a thin dusty seam. This seam, however, did not interrupt crystal growth as shown by crystal habits (cf. Fig. 4/6, crossed nicols). Only thicker and more silty covers (arrows) inhibited and stopped the growth of the fibrous crystals. Large radiaxial fibrous crystals exhibiting typical twin lamellae fill the relic pore space. Sample 12/42. Parallel nicols. Width of the photograph 3 mm.

Fig. 6: Same sample as Fig. 4/5. Crossed nicols. Width of the photograph 3 mm.

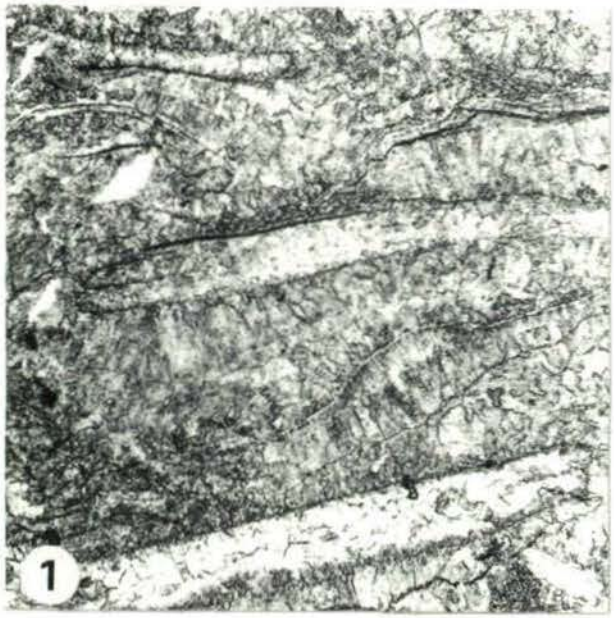
1

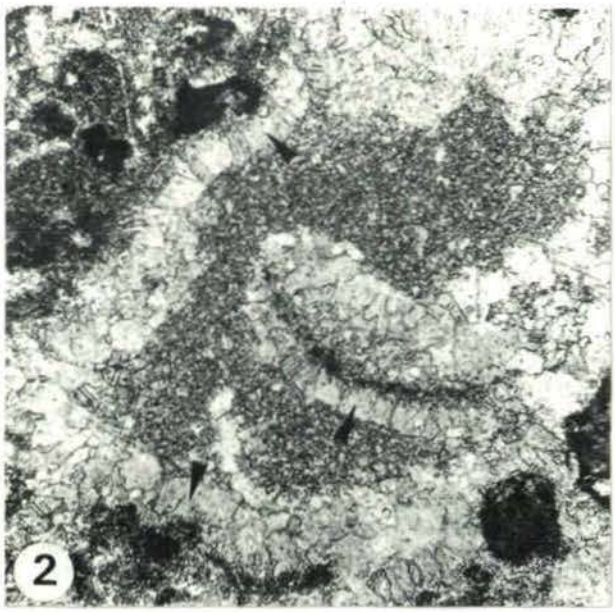
2

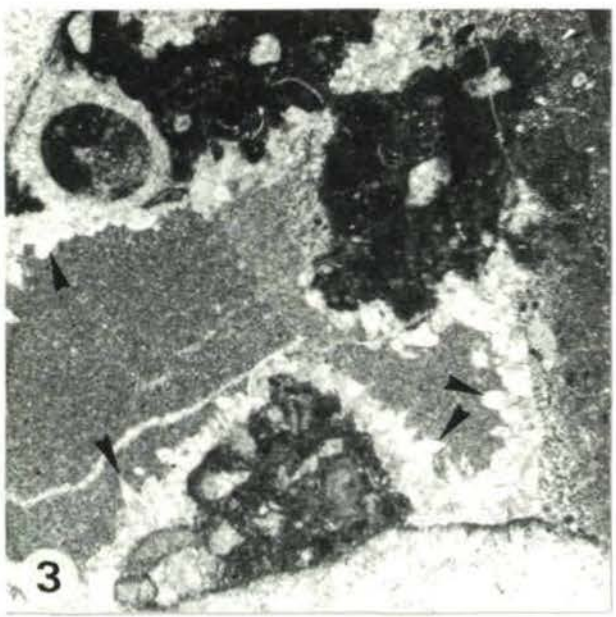
3

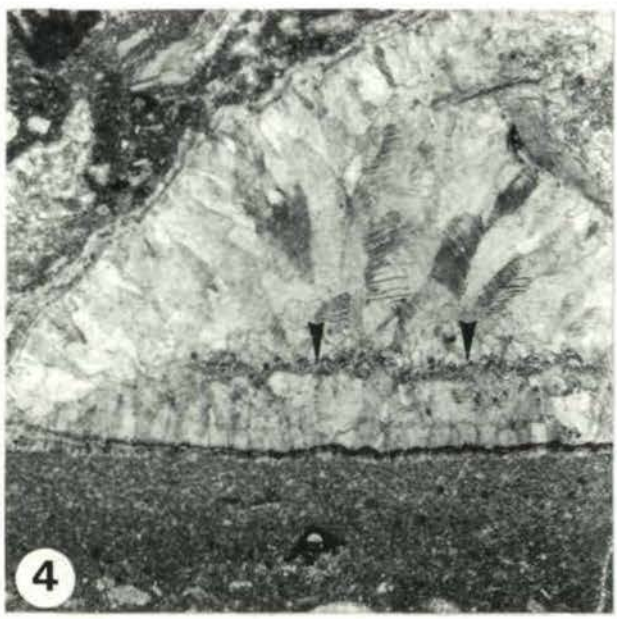
4

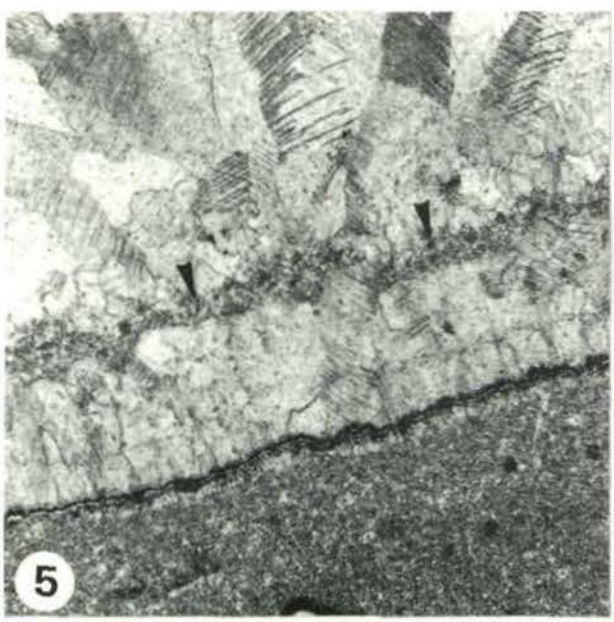
5

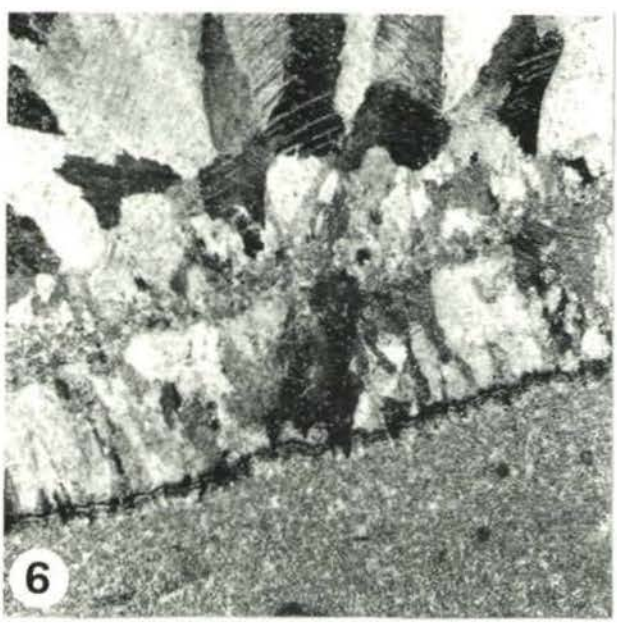
6